

°C and monitored by ^1H NMR spectroscopy. No reaction was observed after 6 days.

Reaction 3e with $\text{H}_2\text{NSi}(\text{CMe}_3)_2\text{Me}_2$. An NMR tube was charged with metallacycle **3e** (7.0 mg , $1.32 \times 10^{-5}\text{ mol}$), $\text{H}_2\text{NSi}(\text{CMe}_3)_2\text{Me}_2$ (3.8 mg , $2.90 \times 10^{-5}\text{ mol}$, 2.2 equiv), and 0.7 mL of C_6D_6 . The solution was degassed, and the NMR tube was flame sealed. The solution was heated at $95\text{ }^\circ\text{C}$, and the reaction was monitored by ^1H NMR spectrometry. After 4 days the conversion of metallacycle **3e** to diphenylacetylene and bisamide **1e** was observed to be complete with no other products formed. The reaction was also found to proceed at $45\text{ }^\circ\text{C}$, requiring several weeks for completion.

General Procedure for the Determination of Catalytic Turnover Rates. An NMR tube was charged with alkyne ($2 \times 10^{-4}\text{ mol}$), amine ($2 \times 10^{-4}\text{ mol}$), the catalyst (8×10^{-6} , $3\text{ mol } \%$), ferrocene internal standard, and 0.7 mL of C_6D_6 . The solution was degassed, and the NMR tube was flame sealed. The reaction was heated at $110\text{ }^\circ\text{C}$ and monitored by ^1H NMR spectrometry. The concentration of product was determined by integration against the internal standard ferrocene. In the cases where both imine and enamine were observed the product concentration was taken to be the sum of the imine and enamine concentrations.

Isomerization of 7a with I_2 . An NMR tube was charged with enamine **7a** (10.6 mg , $3.54 \times 10^{-5}\text{ mol}$), iodine (0.3 mg , $1.18 \times 10^{-6}\text{ mol}$, 0.03 equiv), and 0.7 mL of C_6D_6 . The tube was placed in room light for 1

h, and then a ^1H NMR spectrum was taken which indicated complete conversion to imine had taken place.

Acknowledgment. We are grateful for financial support of this work from the National Institutes of Health (Grant No. GM25457). We would like to thank Dr. F. J. Hollander, Director of the U.C. Berkeley X-ray Diffraction Facility (CHEXRAY), for solving the structures of **3a** and **7a**.

Registry No. **1a**, 117939-64-7; **1b**, 138313-32-3; **1c**, 138313-33-4; **1d**, 117939-63-6; **1e**, 138313-34-5; **2a**, 117939-53-4; **2b**, 117939-51-2; **2c**, 138313-35-6; **2d**, 117939-52-3; **2e**, 138333-46-7; **3a**, 117939-60-3; **3e**, 138313-36-7; **4a**, 138313-37-8; **5a**, 138313-38-9; **6a**, 138313-39-0; **7a**, 138313-30-1; **8a**, 138313-31-2; **10**, 138313-40-3; $\text{Cp}_2\text{Zr}(\text{Me})(\text{Cl})$, 1291-45-8; $\text{LiNH}(2,6\text{-Me}_2\text{C}_6\text{H}_3)$, 111749-95-2; $\text{PhC}\equiv\text{CPh}$, 501-65-5; *p*-Tol-C \equiv C-Tol-*p*, 2789-88-0; $(2,6\text{-Me}_2\text{C}_6\text{H}_3)\text{NH}_2$, 87-62-7; $\text{CH}_2=\text{C}=\text{CH}_2$, 463-49-0; $\text{Me}_2\text{C}=\text{N}(2,6\text{-Me}_2\text{C}_6\text{H}_3)$, 85384-97-0; $\text{H}_2\text{NSi}(\text{CMe}_3)_2\text{Me}_2$, 41879-37-2; acetone, 67-64-1.

Supplementary Material Available: Tables of distances, angles, and x , y , z coordinates from the structure determinations of complexes **3a** and **7a** (10 pages). Ordering information is given on any current masthead page.

Photochemical Substitution Reactions of $[\text{CpFe}(\text{CO})_2]_2$ ($\text{Cp} = \eta^5\text{-C}_5\text{H}_5$) in Hydrocarbon and Tetrahydrofuran Solution at Room Temperature: A Mechanistic Study with Time-Resolved Infrared Spectroscopy

Andrew J. Dixon, Michael W. George, Catherine Hughes, Martyn Poliakoff,* and James J. Turner*

Contribution from the Department of Chemistry, University of Nottingham, Nottingham, England NG7 2RD. Received August 7, 1991

Abstract: Microsecond and nanosecond time-resolved IR spectroscopy (TRIR) have been used to investigate both the kinetics and the nature of the intermediates in the photochemical substitution reactions of $[\text{CpFe}(\text{CO})_2]_2$ ($\text{Cp} = \eta^5\text{-C}_5\text{H}_5$) with THF and $\text{P}(\text{OR})_3$ ($\text{R} = \text{Me}$, Et , and ^iPr) in cyclohexane and *n*-heptane solutions at $25\text{ }^\circ\text{C}$. An important feature of these experiments has been the use of both UV and visible photolysis wavelengths to distinguish between processes involving photoejection of CO, which principally occurs on UV irradiation, and homolysis of the Fe-Fe bond, which is promoted by both UV and visible light. TRIR signals from the depletion of $[\text{CpFe}(\text{CO})_2]_2$ with 308-nm photolysis are used to determine the branching ratio (0.9:1) between homolysis of the Fe-Fe bond and photoejection of CO. These data then permit the evaluation of the IR extinction coefficient of the antisymmetric $\nu(\text{C}-\text{O})$ band of the Fp radical, $\text{CpFe}(\text{CO})_2$, and hence the rate constant for dimerization of Fp. High-resolution microsecond TRIR based on a continuously tunable IR diode laser calibrated by FTIR is used to show that, contrary to previous work, there is no significant difference in wavenumber of the $\nu(\text{C}-\text{O})$ band of the Fp radical between microsecond and picosecond TRIR experiments. UV photolysis of $[\text{CpFe}(\text{CO})_2]_2$ in the presence of THF provides TRIR evidence for the formation of a previously unknown species, $\text{Cp}_2\text{Fe}_2(\text{CO})_3(\text{THF})$, the formation of which involves neither Fp nor $\text{Cp}_2\text{Fe}_2(\mu\text{-CO})_3$ and may well occur via a very short-lived and so far undetected precursor to $\text{Cp}_2\text{Fe}_2(\mu\text{-CO})_3$. TRIR experiments on the reaction of $[\text{CpFe}(\text{CO})_2]_2$ with $\text{P}(\text{OMe})_3$ reveal a very rapid substitution of one CO group in the Fp radical by $\text{P}(\text{OMe})_3$ followed by dimerization of $\text{CpFe}(\text{CO})\text{P}(\text{OMe})_3$ to form $[\text{CpFe}(\text{CO})\text{P}(\text{OMe})_3]_2$. Similar results were obtained with $\text{P}(\text{OEt})_3$ and $\text{P}(\text{O}^i\text{Pr})_3$, although in these cases the $[\text{CpFe}(\text{CO})\text{P}(\text{OR})_3]_2$ compounds are labile and had not previously been detected. It is suggested that an IR band of an intermediate in these reactions, previously attributed to $\text{CpFe}(\text{CO})_2(\mu\text{-CO})\text{CpFe}(\text{CO})\text{P}(\text{O}^i\text{Pr})_3$, is in fact due to $[\text{CpFe}(\text{CO})\text{P}(\text{O}^i\text{Pr})_3]_2$. An overall scheme is given for the reactions, in which all of steps can be explained on the basis of three intermediates, $\text{Cp}_2\text{Fe}_2(\mu\text{-CO})_3$, $\text{CpFe}(\text{CO})_2$, and $\text{CpFe}(\text{CO})\text{P}(\text{OR})_3$; rate constants have been evaluated for most of the steps.

Introduction

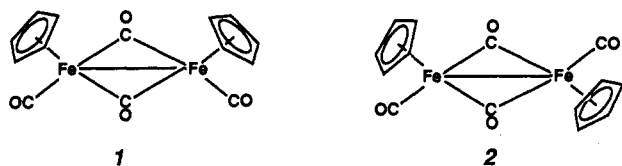
The dinuclear iron complex, $[\text{CpFe}(\text{CO})_2]_2$ ($\text{Cp} = \eta^5\text{-C}_5\text{H}_5$), has been the subject of chemical interest for many years, yet its behavior continues to yield surprises. Initial studies¹ focused on the solvent-dependent equilibrium between *cis* and *trans* isomers,

1 and **2**, and NMR spectroscopy was used to unravel the dynamics of the interconversion between these isomers,² one of the first examples of fluxionality in polynuclear organometallics. More recently, workers have concentrated on the rich photochemistry

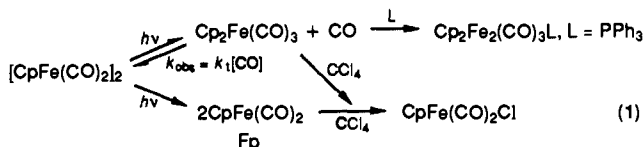
(1) Manning, A. R. *J. Chem. Soc. A* 1968, 1319; McArdle, P. A.; Manning, A. R. *J. Chem. Soc. A* 1969, 1948.

(2) Bullitt, J. G.; Cotton, F. A.; Marks, T. J. *J. Am. Chem. Soc.* 1970, 92, 2155. Gansow, O. A.; Burke, A. R.; Vernon, W. D. *J. Am. Chem. Soc.* 1972, 94, 2550; 1976, 98, 5817.

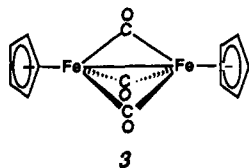
of $[\text{CpFe}(\text{CO})_2]_2$ and related compounds, where a diversity of reaction pathways leads to mononuclear, dinuclear, and even ionic products.³ Indeed, relatively few organometallic compounds have been studied in as much photochemical detail as $[\text{CpFe}(\text{CO})_2]_2$.



Pioneering UV-vis flash photolysis studies by Caspar and Meyer⁴ showed that, on a microsecond time scale, there are two primary photochemical pathways: (i) loss of CO to generate a dinuclear intermediate, $\text{Cp}_2\text{Fe}_2(\text{CO})_3$, and (ii) homolysis of the Fe-Fe bond to form two $\text{CpFe}(\text{CO})_2$ radicals, Fp, see eq 1.



Subsequent matrix isolation experiments revealed the formation of $\text{Cp}_2\text{Fe}_2(\text{CO})_3$ both in solid CH_4 or PVC films⁵ at 20 K and hydrocarbon glasses⁶ at 77 K, and, under these conditions, $\text{Cp}_2\text{Fe}_2(\text{CO})_3$ had a visible absorption band similar in position to that reported by Caspar and Meyer.⁴ Rest and co-workers showed by elegant use of IR spectroscopy and ^{13}C isotopes that all three CO groups in matrix-isolated $\text{Cp}_2\text{Fe}_2(\text{CO})_3$, **3**, were equivalent and bridging.⁵ This was strikingly confirmed by the isolation and X-ray characterization⁷ of $(\text{C}_5\text{Me}_5)_2\text{Fe}_2(\mu\text{-CO})_3$, where the presence of the Me groups stabilizes an otherwise highly reactive intermediate. An interesting feature of these matrix experiments^{5,6} was that $\text{Cp}_2\text{Fe}_2(\text{CO})_3$ appeared to be formed exclusively from the trans isomer of $[\text{CpFe}(\text{CO})_2]_2$; the cis isomer was apparently unaffected under these conditions.⁸



The past decade has seen the rapid development of time-resolved IR spectroscopy,⁹ TRIR, a combination of UV or visible flash photolysis with fast IR detection, originally on a microsecond^{10,11} but now on nanosecond,⁹ picosecond,^{12,13} or even femtosecond¹⁴ time scales. A number of factors made $[\text{CpFe}(\text{CO})_2]_2$ an ideal test compound for the development of TRIR experiments in solution; these factors included good IR data from the matrix iso-

Table I. Wavenumbers, cm^{-1} , of $[\text{CpFe}(\text{CO})_2]_2$ and Its Photoproducts in *n*-Heptane and Cyclohexane^a Solution at Room Temperature

species	wavenumber	assignment
$[\text{CpFe}(\text{CO})_2]_2^b$	2006.6 (2004.4)	$\nu(\text{C-O})_{\text{terminal}}(\text{cis})$
	1961.2 (1960.1)	$\nu(\text{C-O})_{\text{terminal}}(\text{cis/trans})$
	1793.8 (1793.2)	$\nu(\text{C-O})_{\text{bridging}}(\text{cis/trans})$
$\text{CpFe}(\text{CO})_2$	2007 ^c	$a' \nu(\text{C-O})_{\text{terminal}}$
	1935.0 ^d (1933.4) ^d	$a'' \nu(\text{C-O})_{\text{terminal}}$
$\text{Cp}_2\text{Fe}_2(\mu\text{-CO})_3$	1823 ^e (1810) ^e	$e \nu(\text{C-O})_{\text{bridging}}$
$\text{Cp}_2\text{Fe}_2(\text{CO})_3(\text{THF})^{\text{f,g}}$	1969	$\nu(\text{C-O})_{\text{terminal}}$
	1944	$\nu(\text{C-O})_{\text{terminal}}$
	1747	$\nu(\text{C-O})_{\text{bridging}}$

^a Wavenumbers for cyclohexane in parentheses. ^b Wavenumbers from FTIR spectra $\pm 0.1 \text{ cm}^{-1}$. ^c TRIR, CO laser; wavenumbers $\pm 2 \text{ cm}^{-1}$. ^d TRIR, continuously tunable diode laser, wavenumbers $\pm 0.2 \text{ cm}^{-1}$. ^e PVC film 20 K, see ref 5. ^f Solvent; 90% cyclohexane, 10% THF.

Table II. Wavenumbers, cm^{-1} , of Some of the Photoproducts Generated by Photolysis of $[\text{CpFe}(\text{CO})_2]_2$ in the Presence of Phosphites in Cyclohexane Solution

species	wavenumber ^a	assignment
$\text{CpFe}(\text{CO})\text{P}(\text{OMe})_3$	1907	$\nu(\text{C-O})_{\text{terminal}}$
$\text{CpFe}(\text{CO})\text{P}(\text{O}^i\text{Pr})_3$	1904	$\nu(\text{C-O})_{\text{terminal}}$
$\text{CpFe}(\text{CO})\text{P}(\text{OEt})_3$	1907	$\nu(\text{C-O})_{\text{terminal}}$
$\text{Cp}_2\text{Fe}_2(\text{CO})_3\text{P}(\text{OMe})_3^b$	1755 (1752) ^c	$\nu(\text{C-O})_{\text{bridging}}$
$\text{Cp}_2\text{Fe}_2(\text{CO})_3\text{P}(\text{OEt})_3^b$	1751 (1749) ^c	$\nu(\text{C-O})_{\text{bridging}}$
$\text{Cp}_2\text{Fe}_2(\text{CO})_3\text{P}(\text{O}^i\text{Pr})_3^b$	1755 (1753) ^c	$\nu(\text{C-O})_{\text{bridging}}$
$[\text{CpFe}(\text{CO})\text{P}(\text{OMe})_3]_2$	1714 (1714) ^d	$\nu(\text{C-O})_{\text{bridging}}$
$[\text{CpFe}(\text{CO})\text{P}(\text{O}^i\text{Pr})_3]_2$	1720	$\nu(\text{C-O})_{\text{bridging}}$
$[\text{CpFe}(\text{CO})\text{P}(\text{OEt})_3]_2$	1714	$\nu(\text{C-O})_{\text{bridging}}$

^a TRIR, CO laser; wavenumbers $\pm 2 \text{ cm}^{-1}$. ^b $\nu(\text{C-O})_{\text{bridging}}$ only. The single $\nu(\text{C-O})_{\text{terminal}}$ band lies close to that of $[\text{CpFe}(\text{CO})_2]_2$ and is not resolved in the TRIR experiments. ^c Reported wavenumbers (Haines, R. J.; du Preeze, A. L. *Inorg. Chem.* 1969, 8, 1459). ^d Reported wavenumbers from ref 21.

lation experiments^{5,6} and, in the absence of added reactants, the complete reversibility^{4,15} of the photolysis of $[\text{CpFe}(\text{CO})_2]_2$. Even though TRIR measurements are generally more difficult to make than those involving transient UV-visible absorptions, TRIR has considerable advantages in studying a system as complex as $[\text{CpFe}(\text{CO})_2]_2$ because (i) $\nu(\text{C-O})$ IR bands of metal carbonyls frequently provide structural information about the intermediates and (ii) unlike UV-vis absorptions, the $\nu(\text{C-O})$ IR bands are relatively narrow with little overlap between bands of different species in solution.¹⁶ Thus IR spectroscopy can, for example, distinguish between cis and trans isomers of $[\text{CpFe}(\text{CO})_2]_2$, while UV spectroscopy cannot. A particularly important feature of the TRIR equipment at Nottingham is that it has been designed to study substitution reactions and so most signals can be obtained "single shot". In addition, unlike conventional UV-vis flash photolysis where the same solution is often used for many shots, the TRIR reactant solution is held in a flow-cell and can be changed between each shot.^{9,17}

Microsecond TRIR experiments¹¹ have confirmed Caspar and Meyer's observation⁴ of two primary photochemical pathways for $[\text{CpFe}(\text{CO})_2]_2$, loss of CO and homolysis of the Fe-Fe bond. The $\nu(\text{C-O})$ IR band of $\text{Cp}_2\text{Fe}_2(\text{CO})_3$ was close in wavenumber to that observed in matrix experiments, and the two $\nu(\text{C-O})$ bands of the Fp radical were identified for the first time, see Table I. However, unlike the matrix experiments, the TRIR spectra in solution showed depletion of both cis and trans isomers of $[\text{CpFe}(\text{CO})_2]_2$

(15) Moore, B. D.; Poliakoff, M.; Turner, J. J. *J. Am. Chem. Soc.* 1986, 108, 1819.

(16) This advantage becomes rather less apparent on a picosecond time scale, where the presence of vibrationally excited species causes considerable broadening of the IR bands.¹²⁻¹⁴ For a general overview of the latest work in this area, see: *Proceedings of the 5th International Conference on Time-Resolved Vibrational Spectroscopy*; Tokyo, Japan, 1991.

(17) Dixon, A. J.; Healy, M. A.; Hodges, P. M.; Moore, B. D.; Poliakoff, M.; Simpson, M. B.; Turner, J. J.; West, M. A. *J. Chem. Soc., Faraday Trans. 2* 1986, 82, 2083.

(3) Meyer, T. J.; Caspar, J. V. *Chem. Rev.* 1985, 85, 187.

(4) Caspar, J. V.; Meyer, T. J. *J. Am. Chem. Soc.* 1980, 102, 7794.

(5) (a) Hooker, R. H.; Mahmoud, K. A.; Rest, A. J. *J. Chem. Soc., Chem. Commun.* 1983, 1022. (b) For more recent matrix photochemistry of related compounds, see: Hooker, R. H.; Rest, A. J. *J. Chem. Soc., Dalton Trans.* 1990, 1221.

(6) Hepp, A. F.; Blaha, J. P.; Lewis, C.; Wrighton, M. S. *Organometallics* 1984, 3, 174.

(7) Blaha, J. P.; Bursten, B. E.; Dewan, J. C.; Frankel, R. B.; Randolph, C. W.; Wilson, B. A.; Wrighton, M. S. *J. Am. Chem. Soc.* 1985, 107, 4561.

(8) The so-called "matrix cage effect" probably prevents the observation of the Fp radical in such experiments because, even if formed, the radicals would be too large to move apart in the matrix and would therefore recombine.

(9) (a) Poliakoff, M.; Weitz, E. *Adv. Organomet. Chem.* 1986, 25, 277.

(b) Grevels, F.-W.; Klotzbücher, W. E.; Schaffner, K. *Chem. Rev.*, in press.

(10) Hermann, H.; Grevels, F.-W.; Henne, A.; Schaffner, K. *J. Phys. Chem.* 1982, 86, 5151.

(11) Moore, B. D.; Simpson, M. B.; Poliakoff, M.; Turner, J. J. *J. Chem. Soc., Chem. Commun.* 1984, 972.

(12) Moore, J. N.; Hansen, P. A.; Hochstrasser, R. M. *J. Am. Chem. Soc.* 1989, 111, 4563.

(13) Wang, L.; Zhu, X.; Spears, K. G. *J. Am. Chem. Soc.* 1988, 110, 8695.

(14) Anfirud, P. A.; Han, C.-H.; Lian, T.; Hochstrasser, R. M. *J. Phys. Chem.* 1991, 95, 574.

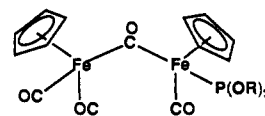
on this time scale, possibly because $\text{cis} \rightleftharpoons \text{trans}$ interconversion is relatively rapid on this timescale.² In addition, the photolysis of $[\text{CpFe}(\text{CO})_2]_2$ was found to be wavelength dependent with almost no CO loss during visible photolysis, $\lambda > 600 \text{ nm}$; two wavelength photolysis experiments¹⁷ (UV followed by visible) showed that this effect was a genuine wavelength difference in primary photochemistry¹⁸ and not merely due to secondary photolysis of $\text{Cp}_2\text{Fe}_2(\text{CO})_3$.

The photolysis of $[\text{CpFe}(\text{CO})_2]_2$ with visible light has formed the basis of some ingenious picosecond¹² and femtosecond¹⁴ TRIR experiments by Hochstrasser and co-workers. Although primarily designed to probe molecular dynamics in solution, these experiments appeared to show interesting differences from the microsecond TRIR results. In particular, picosecond measurements¹² indicated a $\nu(\text{C}-\text{O})$ band ca. 5 cm^{-1} lower than the value reported^{11,17} for the antisymmetric $\nu(\text{C}-\text{O})$ absorption of the Fp radical. This shifted band was tentatively assigned¹² to the formation of a very short-lived intermediate formed prior to homolysis of the Fe-Fe bond.

As well as probing the primary photochemistry, spectroscopic techniques have been widely used to study substitution reactions of $[\text{CpFe}(\text{CO})_2]_2$ (see, e.g., eq 1). Microsecond and nanosecond TRIR experiments^{19,20} have provided valuable data about processes such as the reaction of $\text{Cp}_2\text{Fe}_2(\text{CO})_3$ with CH_3CN and a range of alkyl phosphines to form the corresponding $\text{Cp}_2\text{Fe}_2(\text{CO})_3\text{L}$ complexes. Although the enthalpy of activation, ΔH^\ddagger , was similar for all of these ligands, there was a systematic change in the entropy of activation, ΔS^\ddagger , with a corresponding decrease in the bimolecular rate constant with increasing cone angle of the phosphine.¹⁹ Under these conditions, Fp radicals did not react with phosphines at a measurable rate¹⁹ but merely recombined rapidly to regenerate $[\text{CpFe}(\text{CO})_2]_2$. On the other hand, Fp reacted with $\text{P}(\text{OMe})_3$ to form $\text{CpFe}(\text{CO})\text{P}(\text{OMe})_3$ at a rate close to the diffusion-controlled limit,²⁰ a step of considerable importance to the reactions considered in this paper.

The reaction of $[\text{CpFe}(\text{CO})_2]_2$ with alkyl phosphites has aroused considerable interest, particularly the reaction with $\text{P}(\text{OMe})_3$. The reason for this interest is that, unlike other phosphites or phosphines, photochemical reaction ($\lambda > 500 \text{ nm}$) of $\text{P}(\text{OMe})_3$ with $[\text{CpFe}(\text{CO})_2]_2$, first reported²¹ by Abrahamson et al., leads to the *disubstituted* compound $[\text{CpFe}(\text{CO})\text{P}(\text{OMe})_3]_2$ as the sole product. Tyler and co-workers have since made a detailed study of the photochemical reaction with $\text{P}(\text{O}^i\text{Pr})_3$ in THF or ethyl chloride solutions.²² They observed a yellow intermediate, stable at -78°C ($[\text{CpFe}(\text{CO})_2]_2$ is red and $\text{Cp}_2\text{Fe}_2(\text{CO})_3\text{P}(\text{O}^i\text{Pr})_3$ is green). This intermediate had a $\nu(\text{C}-\text{O})$ band at 1720 cm^{-1} , indicating a bridging CO group, but *no* UV-vis absorption in the region 300–400 nm, normally associated with the $\sigma \rightarrow \sigma^*$ transition of an M-M bond in a dimetallic complex.²³ The intermediate decayed when the solution was warmed and the *mono-substituted* complex, $\text{Cp}_2\text{Fe}_2(\text{CO})_3\text{P}(\text{O}^i\text{Pr})_3$, was formed. When $\text{P}(\text{OMe})_3$ was added to a solution of the intermediate before warmup, the final product was $[\text{CpFe}(\text{CO})\text{P}(\text{OMe})_3]_2$. In the absence of added phosphite, $[\text{CpFe}(\text{CO})_2]_2$ did not appear to react photochemically with THF (i.e., the *color* of the solution remained

unchanged²⁴). From the spectroscopic and chemical observations, it was concluded that the yellow intermediate had structure **4**, particularly unusual as it contains a bridging CO group but *no* Fe-Fe bond. Formation of **4** would require a third photochemical



4

pathway, in addition to the formation of $\text{Cp}_2\text{Fe}_2(\text{CO})_3$ and $\text{CpFe}(\text{CO})_2$ so far detected by transient spectroscopy. It is therefore important to establish whether such a pathway does exist, since the results clearly have chemical implications well beyond the reactions of $[\text{CpFe}(\text{CO})_2]_2$ itself.

The aim of this paper is to present a consistent mechanism for the photolysis of $[\text{CpFe}(\text{CO})_2]_2$ and, in particular, its substitution reactions with phosphites. The mechanism is largely built on the basis of TRIR data obtained in our laboratory. The overall strategy has been to exploit the known wavelength dependence of the photochemistry to establish the precise role of the Fp radical in these reactions. The results are divided into three parts.

(i) **Characterization of the Fp Radical.** The first part consists of measurement of the branching ratio between the CO loss and bond homolysis pathways during 308-nm photolysis, estimation of the IR extinction coefficient of the Fp radical, and accurate measurement of the wavenumber of $\nu(\text{C}-\text{O})$ bands with use of our newly developed high-resolution tunable IR diode laser TRIR equipment; measurements which indicate that differences between microsecond and picosecond TRIR results are probably not significant.

(ii) **Role of THF.** The second part consists of TRIR detection of $\text{Cp}_2\text{Fe}_2(\text{CO})_3(\text{THF})$, competition with formation of $\text{Cp}_2\text{Fe}_2(\text{CO})_3$, and evidence for the existence of a very short-lived but undetected precursor to $\text{Cp}_2\text{Fe}_2(\text{CO})_3$, generated by UV but not visible photolysis.

(iii) **TRIR in Phosphite Substitution Reactions.** The third part consists of TRIR experiments with $[\text{CpFe}(\text{CO})_2]_2$ and $\text{Cp}_2\text{Fe}_2(\text{CO})_3\text{P}(\text{OMe})_3$ in the presence of $\text{P}(\text{OMe})_3$, evidence for Fp and $\text{Cp}_2\text{Fe}_2(\text{CO})_3$ as the important reaction intermediates in all reactions, and observation of previously undetected and highly labile *disubstituted* species $[\text{CpFe}(\text{CO})\text{P}(\text{O}^i\text{Pr})_3]_2$ with $\nu(\text{C}-\text{O})$ very close to that attributed to **4**.

Experimental Section

(Note, wherever possible, rate constants have been given the same numbering as the equation which defines them. Thus k_4 is defined in eq 4, etc.)

The operating principles of our point-by-point TRIR spectrometer have been discussed in some detail previously.^{9a,15} Briefly, a reaction is initiated by a pulsed UV or visible source (flash lamp or laser) and a CW IR laser is used to monitor transient changes in IR absorption at one particular IR wavelength. All of the TRIR spectrometers used in this paper have AC-coupled detectors which only record *changes* in IR absorption. Thus, absorptions which remain constant, such as those due to the solvent, do not register at all. The digitized signal is stored for further processing. The wavelength of the IR monitoring laser is then changed, and the UV flash is repeated. The process is repeated until data have been accumulated right across the IR region of interest. The stored kinetic traces are then used to reconstruct IR difference spectra corresponding to various time delays after the flash. In such spectra, positive peaks are due to species created by the flash and negative peaks are due to those destroyed by the flash. However, this procedure often leads to rather complicated spectra, particularly when there are several intermediates in a reaction. Fortunately, because there was little overlap of absorption bands in the experiments presented here, it has been possible to simplify most of the spectra by omitting the negative traces due to depletion of the starting material, without seriously impairing the information content of the spectra.

The majority of TRIR measurements reported in this paper were made with a TRIR spectrometer based on an Edinburgh Instruments PL3 CW CO IR laser, modified for cooling to -110°C by a Polycold

(18) A similar wavelength dependence has been demonstrated in the photochemistry of other dinuclear species. (Yesaka, H.; Kobayashi, T.; Yasufuku, K.; Nagakuru, S. *J. Am. Chem. Soc.* **1983**, *105*, 6249. Van Vliet-berge, B. A.; Abrahamson, H. B. *J. Photochem. Photobiol.* **1990**, *52*, 69).

(19) Dixon, A. J.; Healy, M. A.; Poliakoff, M.; Turner, J. J. *J. Chem. Soc., Chem. Commun.* **1986**, 994. This communication contains, inter alia, a very brief report of the observation of $\text{Cp}_2\text{Fe}_2(\text{CO})_3(\text{THF})$ by TRIR.

(20) Dixon, A. J.; Gravelle, S. A.; van der Burgt, L. J.; Poliakoff, M.; Weitz, E. *J. Chem. Soc., Chem. Commun.* **1987**, 1023.

(21) Abrahamson, H. B.; Palazzotto, M. C.; Reichel, C. L.; Wrighton, M. S. *J. Am. Chem. Soc.* **1979**, *101*, 4123.

(22) (a) Tyler, D. R.; Schmidt, M. A.; Gray, H. B. *J. Am. Chem. Soc.* **1979**, *101*, 2653. (b) Tyler, D. R., et al. *J. Am. Chem. Soc.* **1983**, *105*, 6018. (c) Stiegman, A. E.; Tyler, D. R. *Acc. Chem. Res.* **1984**, *17*, 61.

(23) There has been considerable argument whether the $\sigma \rightarrow \sigma^*$ assignment, originally propounded for compounds without bridging CO groups, applies equally to such bridged species where some Authors prefer a $\pi \rightarrow \pi^*$ assignment.³ However the precise assignment of this band is not crucial to the conclusions of this paper.

(24) Tyler, D. R., personal communication.

cryocooler. The CO laser has an IR range of 2010–1600 cm^{-1} , tunable in steps of ca. 4 cm^{-1} and calibrated ($\pm 1 \text{ cm}^{-1}$) with a Perkin-Elmer Model 283 IR spectrophotometer. IR signals were measured with liquid nitrogen cooled MCT detectors (photoconductive New England Research Center MPC4, ca. 1 μs response). Higher resolution TRIR spectra were obtained with a Mutek tunable IR diode laser (Model MDS 1100) fitted with a Mutek Model MDS 1200 monochromator and a custom-built Mutek "Experiment" module with optics matched to our IR cell.^{25,26} Unlike the CO laser, the IR diode laser is continuously tunable, but laser output occurs at a number of closely spaced frequencies, one of which is isolated by the monochromator for the TRIR experiment. In order to exploit the tunability of the diode laser for high-resolution TRIR of solutions, precise wavelength measurement is crucial, and this was achieved by diverting the beam into a Nicolet Model 7199 FTIR interferometer (0.06 cm^{-1} resolution) with Nicolet 1280 computer.²⁷

Our original TRIR spectrometer was based on an Applied Photo-physics 100J Xe flash lamp (ca. 15 μs FWHM), which could be fitted with Wratten filters to exclude UV light as required.¹⁵ Most of the experiments described in this paper were carried out with a Lumonics HyperEx 440 XeCl excimer laser (308 nm, ca. 100 mJ, 30 ns pulse) which pumped an Oxford Instruments EDL1 dye laser (rhodamine 6G, <10 mJ) as required.^{25,28}

Data were collected on a Datalab DL902 transient digitizer or a Gould Model 4072 digitizer and stored on BBC "Master" computers. Raw data were collected as a voltage signal from the detector and were converted to "% absorption" after using a mechanical shutter to measure the voltage corresponding to 100% absorption of the laser light, usually in the range 2–5 V. Subsequent data analysis and spectral manipulation were performed on a BBC Archimedes A3000 RISC microcomputer with software developed in Nottingham.^{25,28a,29} Most experiments with the CO laser were recorded "single shot"; those with the diode laser were averaged over a modest number of shots as detailed in the text. Some measurements were made on the TRIR equipment (CO laser, InSb detector, XeF laser) at Northwestern University³⁰ which has a better time resolution of ca. 30 ns but required modest averaging (16 shots) on all measurements.

$[\text{CpFe}(\text{CO})_2]_2$ (various sources) was purified by recrystallization; $\text{Cp}_2\text{Fe}_2(\text{CO})_3\text{P}(\text{OMe})_3$ was prepared by reaction of $\text{P}(\text{OMe})_3$ with $\text{Cp}_2\text{Fe}_2(\text{CO})_3\text{CH}_3\text{CN}$, which was made by literature methods.³⁰ Cyclohexane and *n*-heptane (both Aldrich HPLC Grade) were dried by distillation over CaH_2 and tetrahydrofuran (THF, Aldrich) was distilled over Na. All solutions were degassed by dynamic pumping.²⁹ $\text{P}(\text{OMe})_3$, $\text{P}(\text{O}^i\text{Pr})_3$, and other phosphites were used as supplied. Research grade gases, Ar (Messer Griesheim), and CO (BOC) were used without further purification. Routine IR spectra were obtained with a Nicolet MX3600 interferometer and Nicolet 1280 computer.

Results and Discussion

Characterization of the $\text{CpFe}(\text{CO})_2$ Radical (Fp). Quantum yields have been measured²¹ for the 366-nm photolysis of $[\text{CpFe}(\text{CO})_2]_2$; substitution by PPh_3 was found to have a lower quantum yield (0.05 in C_6H_6) than that for formation of $\text{CpFe}(\text{CO})_2\text{Cl}$ (0.23 in CCl_4).³¹ It is difficult to compare these quantum yields directly³ because they were obtained in different solvents. Furthermore, one cannot easily correlate these quantum yields with the two primary photochemical pathways, because both the Fp radical and $\text{Cp}_2\text{Fe}_2(\text{CO})_3$ apparently react⁴ with CCl_4 . TRIR, however, provides a convenient means of measuring the branching ratio between the loss of CO and homolysis of the Fe–Fe bond. Figure 1 shows a kinetic TRIR trace recorded at the wavelength

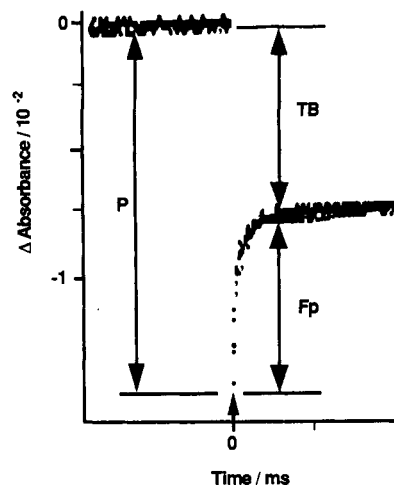


Figure 1. TRIR kinetic trace recorded at 1788.5 cm^{-1} , obtained by UV (308 nm) excimer laser photolysis of $[\text{CpFe}(\text{CO})_2]_2$ (1×10^{-3} M). The trace shows the depletion and bimodal regeneration $[\text{CpFe}(\text{CO})_2]_2$ due to recombination of Fp radicals and $\text{Cp}_2\text{Fe}_2(\text{CO})_3$ with CO. The labels indicate the following: P, the absorbance change due to overall depletion of $[\text{CpFe}(\text{CO})_2]_2$; Fp, the absorbance change due to recombination of the Fp radicals; TB, the residual absorbance, corresponding to the conversion of $[\text{CpFe}(\text{CO})_2]_2$ to $\text{Cp}_2\text{Fe}_2(\text{CO})_3$. (The label "TB" has been derived from the triply-bridging structure of $\text{Cp}_2\text{Fe}_2(\text{CO})_3$, see 3.) In this and subsequent figures, the arrow on the time axis indicates the moment of firing the UV flash.

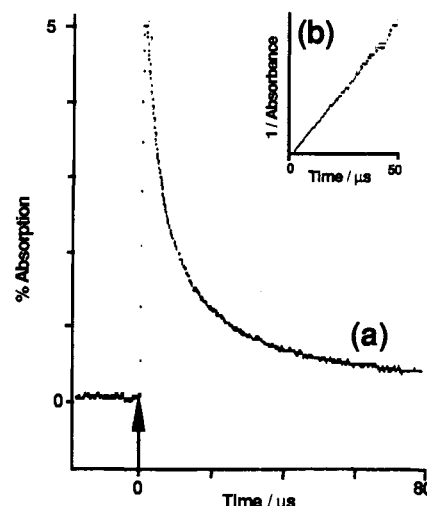


Figure 2. (a) TRIR kinetic trace due to the Fp radical, recorded at 1938 cm^{-1} and (b) inset: plot of $(\text{absorbance})^{-1}$ vs time, showing that the decay of Fp follows second-order kinetics. The kinetic trace was recorded in the same experiment as the trace shown in Figure 1.

of the $\nu(\text{C}-\text{O})$ band due to the bridging CO groups of both the cis and the trans isomers of $[\text{CpFe}(\text{CO})_2]_2$ in cyclohexane.³² On this time scale, the trace shows three distinct features: (i) an instantaneous bleaching caused by flash photolysis of the parent $[\text{CpFe}(\text{CO})_2]_2$, (ii) a region of rapid recovery corresponding to the recombination of the Fp radicals, and (iii) a region of slow recovery corresponding to the much slower recombination of $\text{Cp}_2\text{Fe}_2(\text{CO})_3$ with photoejected CO. From the absorbance changes in these three regions of the trace, it can be seen that the ratio of bond homolysis to CO loss is ca. $0.9 \pm 0.1:1$. After allowing for the fact that bond homolysis generates two Fp radicals per molecule of $[\text{CpFe}(\text{CO})_2]_2$ destroyed, the ratio Fp/ Cp_2Fe_2-

(25) George, M. W. Ph.D. Thesis, University of Nottingham, UK, 1990.

(26) Howdle, S. M.; Jobling, M.; George, M. W.; Poliakov, M. *Proceedings of the 2nd International Symposium on Supercritical Fluids (Boston)*; McHugh, M. A., Ed.; Johns Hopkins University: 1991; p 189.

(27) The optical arrangement for this FTIR calibration, to be published in detail elsewhere, was similar to that previously described for calibration of a CO laser (Bristow, N. J. Ph.D. Thesis, University of Nottingham, UK, 1985).

(28) (a) Hodges, P. M. Ph.D. Thesis, University of Nottingham, UK, 1988.

(b) Glyn, P. Ph.D. Thesis, University of Nottingham, UK, 1991.

(29) Dixon, A. J. Ph.D. Thesis, University of Nottingham, UK, 1989.

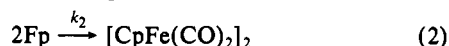
(30) Labinger, J. A.; Madhavan, S. *J. Organomet. Chem.* 1977, 134, 381.

(31) These quantum yields²¹ refer to the loss of $[\text{CpFe}(\text{CO})_2]_2$. Tyler et al.^{22b} obtain values which are consistently somewhat higher. The quantum yield for formation of $\text{CpFe}(\text{CO})_2\text{Cl}$ has been measured²¹ as 0.44, approximately twice the value for the disappearance of $[\text{CpFe}(\text{CO})_2]_2$. It has been reported²¹ that the quantum yield for disappearance of $[\text{CpFe}(\text{CO})_2]_2$ in CCl_4 is greater at 313 than 366 nm, but the corresponding quantum yield for reaction with PPh_3 was not reported, possibly due to UV absorption by the C_6H_6 solvent.

(32) It is important to make the measurement in the $\nu(\text{C}-\text{O})_{\text{bridging}}$ region, where the bands of the cis and trans isomers of $[\text{CpFe}(\text{CO})_2]_2$ coincide, rather than in the $\nu(\text{C}-\text{O})_{\text{terminal}}$ region, where they do not. In this way, one avoids any complications which could arise if the photolysis altered the ratio of cis to trans isomers, as was indeed observed¹⁵ with the UV photolysis of $[(\text{C}_5\text{Me}_5)\text{Fe}(\text{CO})_2]_2$.

(CO)₃ is $1.8 \pm 0.2:1$. This ratio differs considerably from the ratio of quantum yields (0.23:0.05), but the difference probably originates, at least in part, from the difference in photolysis wavelengths (see above; 308 nm for TRIR and 366 nm for the quantum yield³¹).

Figure 2 shows the TRIR trace, from the same experiment as Figure 1, corresponding to the $\nu(\text{C-O})$ absorption of the Fp radical. As expected, the signal decays by a second-order process (see inset plot), consistent with the bimolecular recombination of Fp to regenerate $[\text{CpFe}(\text{CO})_2]_2$, eq 2. However, evaluation of the



second-order rate constant for this process, k_2 , requires a numerical value for the IR extinction coefficient of the Fp radical at this wavenumber. A value of $5 \times 10^3 \text{ M}^{-1} \text{ cm}^{-1}$ can be derived³³ from the known extinction coefficient of $[\text{CpFe}(\text{CO})_2]_2$ and the information contained in Figures 1 and 2. Most gratifyingly, the resulting value of k_2 , $4.5 \pm 2.0 \times 10^9 \text{ M}^{-1} \text{ s}^{-1}$, is the same, within experimental error, as that deduced by Caspar and Meyer, $3 \times 10^9 \text{ M}^{-1} \text{ s}^{-1}$, from their UV-vis flash photolysis experiments.⁴ These rates are slightly larger than the corresponding rate constant, $7 \times 10^8 \text{ M}^{-1} \text{ s}^{-1}$, for the bimolecular recombination of $\text{Mn}(\text{CO})_5$ radicals in cyclohexane³⁴ and close to the diffusion-controlled limit, $4 \times 10^9 \text{ M}^{-1} \text{ s}^{-1}$, under these conditions in cyclohexane.

The Fp radical has been featured in several ultrafast TRIR experiments.^{12,14} As described above, there has been discussion over the apparent shift in the lower frequency $\nu(\text{C-O})$ band which was reported to be 5 cm^{-1} higher in microsecond TRIR spectra¹¹ than in those recorded on shorter time scales.^{12,14,35} Such a difference could have considerable significance as it might indicate the presence of a very short-lived precursor to the Fp radical (e.g., an excited state of $[\text{CpFe}(\text{CO})_2]_2$). However, we now show that the difference is probably not significant, merely arising from differences in lasers and solvents used in the microsecond and picosecond TRIR experiments.

The effect of using different lasers and solvents is apparent from Figure 3. Spectrum (a) illustrates the band of Fp recorded in *n*-heptane with use of a CO laser, tunable in steps of ca. 4 cm^{-1} . Only three of these laser lines (indicated by ■) actually overlap the band, the contour of which has been approximated by computer interpolation (light points).³⁶ Clearly, there is substantial uncertainty in the position of the band maximum. By contrast, Figure 3b shows the same TRIR band recorded with a continuously tunable IR diode laser, accurately calibrated by FTIR. With this laser, all of the points are genuine data points, and the pre-

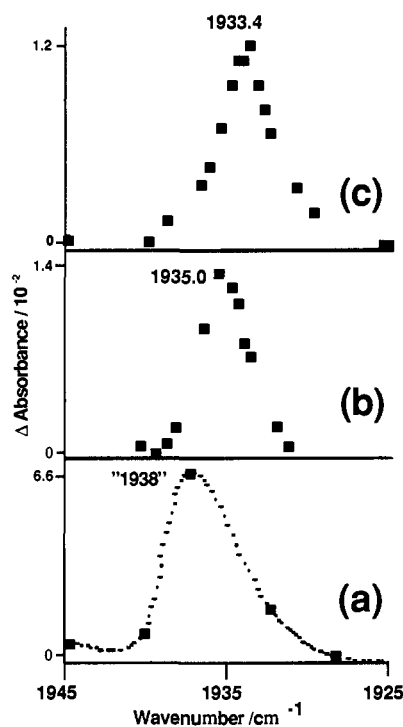


Figure 3. TRIR point-by-point spectra of the antisymmetric $\nu(\text{C-O})$ band of the Fp radical showing the effect of different lasers and solvents on the apparent band maximum. (a) Spectrum in *n*-heptane solution, obtained with a line-tunable CO laser; ■ indicates measured data points. (b) Spectrum in *n*-heptane obtained with a continuously tunable IR diode laser calibrated by FTIR (see Experimental Section); all points are actual data points. (c) IR diode TRIR spectrum in cyclohexane solution showing the solvent shift in the band maximum.

cision in measuring the band maximum is greatly increased. The comparison of microsecond and picosecond TRIR spectra is further confused by differences in solvent; the picosecond experiments were carried out in cyclohexane,¹² while many of the microsecond results¹⁹ were obtained in *n*-heptane, which has less prominent IR bands in this region than does cyclohexane. Conventional FTIR spectra show a small but significant shift in the $\nu(\text{C-O})$ bands of $[\text{CpFe}(\text{CO})_2]_2$ between these two solvents; the $\nu(\text{C-O})_{\text{terminal}}$ bands in cyclohexane are 1.2 cm^{-1} and $\nu(\text{C-O})_{\text{bridging}}$ 0.7 cm^{-1} lower than in *n*-heptane. The IR diode spectrum in Figure 3c shows that the band of Fp in cyclohexane is also shifted by a similar amount (-1.6 cm^{-1}) compared to *n*-heptane and its band maximum (1933.4 cm^{-1}) is exactly coincident with that reported in the picosecond TRIR experiments.¹²

The line width of the band Figure 3c, 3.5 cm^{-1} , is similar to that observed for the $\nu(\text{C-O})_{\text{terminal}}$ bands of the conventional FTIR spectrum of $[\text{CpFe}(\text{CO})_2]_2$ in cyclohexane. Thus, unlike the apparent wavenumber shift, the broadening of the band of Fp in the picosecond TRIR spectrum is both clear-cut and significant, probably the result of vibrational excitation in the "nascent" Fp radical. The relatively long relaxation time of these excited states has been one of the more unexpected results to emerge from picosecond TRIR studies.^{12-14,16} However, the full mechanistic implications of these results will only become clear after more systems have been studied.

Our high-resolution TRIR measurements, therefore, do not support the previously published^{12,14} evidence for the formation of any transient intermediate during the homolysis of the Fe-Fe bond. By contrast, the next section describes the reaction of $[\text{CpFe}(\text{CO})_2]_2$ with THF where TRIR does provide evidence, albeit indirect, for the existence of a very short-lived intermediate prior to the formation of $\text{Cp}_2\text{Fe}_2(\text{CO})_3$.

The Reaction with THF. Figure 4 shows a series of TRIR spectra obtained after the UV flash photolysis of $[\text{CpFe}(\text{CO})_2]_2$ in cyclohexane heavily doped with THF (10% by volume). On this time scale, there are three photoproducts, all generated within

(33) There is a reported value of $6200 \text{ M}^{-1} \text{ cm}^{-1}$ for the molar extinction coefficient of the $\nu(\text{C-O})_{\text{bridging}}$ band of $[\text{CpFe}(\text{CO})_2]_2$ at the band maximum 1792 cm^{-1} (Wrighton, M. S.; Hepp, A. F. *J. Am. Chem. Soc.* **1983**, *105*, 5934). The band is relatively narrow (ca. 4.5 cm^{-1} FWHM). The TRIR measurement in Figure 1 was made at $1788.5 \pm 0.5 \text{ cm}^{-1}$, close to the most sloping part of the band contour, introducing considerable uncertainty into the value of the extinction coefficient appropriate to the TRIR measurement, $1300 \pm 400 \text{ M}^{-1} \text{ cm}^{-1}$. Applying this value to Figure 1 where the pathlength was 1 mm, the absorbance change corresponds to the depletion of $1.1 \times 10^{-4} \text{ M}$ of $[\text{CpFe}(\text{CO})_2]_2$ (i.e., ca. 4% photolysis of the original solution). Given the branching ratio calculated above, this depletion results in the formation of $1.0 \times 10^{-4} \text{ M}$ Fp (and $6 \times 10^{-5} \text{ M}$ $\text{Cp}_2\text{Fe}_2(\text{CO})_3$). From this concentration of Fp and the absorbance change in Figure 2, one obtains $5.0 \pm 1.5 \times 10^3 \text{ M}^{-1} \text{ cm}^{-1}$ as the extinction coefficient at 1938 cm^{-1} for Fp. This value is consistent with the reported value, $1.5 \times 10^3 \text{ M}^{-1} \text{ cm}^{-1}$, for the extinction coefficient of the antisymmetric $\nu(\text{C-O})$ band of $\text{CpFe}(\text{CO})_2\text{H}$ (Norton, J. R.; Sullivan, J. M.; Moore, E. J. *J. Am. Chem. Soc.* **1986**, *108*, 2257). The extinction coefficient of $\text{Cp}_2\text{Fe}_2(\text{CO})_3$ can be evaluated similarly, $7.4 \pm 1.2 \times 10^3 \text{ M}^{-1} \text{ cm}^{-1}$ at 1823 cm^{-1} .

(34) Church, S. P.; Hermann, H.; Grevels, F.-W.; Schaffner, K. *J. Chem. Soc., Chem. Commun.* **1984**, 785. An earlier UV-vis flash photolysis measurement of this rate constant gave a value somewhat larger, $3.9 \times 10^9 \text{ M}^{-1} \text{ s}^{-1}$ (Hughey, J. L.; Anderson, C. P.; Meyer, T. J. *J. Organomet. Chem.* **1977**, *125*, C49).

(35) A band originally reported¹² at 1925 cm^{-1} has recently been assigned to an artefact,¹⁴ such as must inevitably be an occasional feature of such demanding experiments.

(36) Such interpolation can give an almost perfect representation of a relatively broad band (see e.g., Dixon, A. J.; Glyn, P.; Healy, M. A.; Hodges, P. M.; Jenkins, T. J.; Poliakoff, M.; Turner, J. J. *Spectrochim. Acta* **1988**, *44A*, 1309), but it cannot be more than approximate in a case such as that in Figure 3a.

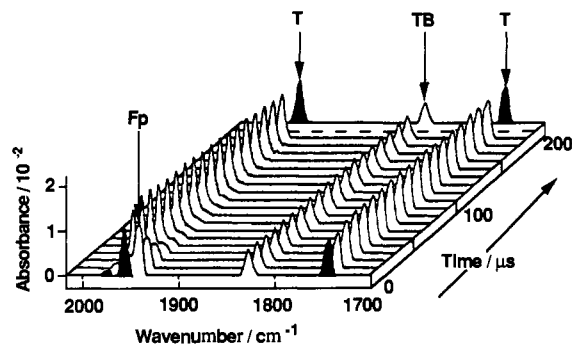


Figure 4. A series of TRIR spectra (Xe flash lamp photolysis) showing the "instantaneous" formation of $\text{Cp}_2\text{Fe}_2(\text{CO})_3(\text{THF})$, bands colored black, during the photolysis of $[\text{CpFe}(\text{CO})_2]_2$ (5×10^{-3} M in 10% THF, 90% cyclohexane solution 0.1 mm optical pathlength). Other bands have been labeled as follows: $\text{CpFe}(\text{CO})_2$, Fp; $\text{Cp}_2\text{Fe}_2(\text{CO})_3$, TB. The depletion of the IR bands of the parent $[\text{CpFe}(\text{CO})_2]_2$ have been omitted (see Experimental Section). Similarly, the penultimate spectrum has been omitted for clarity.

the lifetime of the UV flash: $\text{Cp}_2\text{Fe}_2(\text{CO})_3$, the Fp radical, and a third product with one $\nu(\text{C}-\text{O})_{\text{bridging}}$ and two $\nu(\text{C}-\text{O})_{\text{terminal}}$ bands, colored black in Figure 4, and close in wavenumber³⁷ to those of $\text{Cp}_2\text{Fe}_2(\text{CO})_3(\text{MeCN})$.¹⁹ This third product is not observed in the absence of THF and is reasonably identified as the previously unknown and rather labile compound, $\text{Cp}_2\text{Fe}_2(\text{CO})_3(\text{THF})$. Similar results were obtained in *n*-heptane/THF solutions.

There is clear evidence that the Fp radical is not involved in the formation of $\text{Cp}_2\text{Fe}_2(\text{CO})_3(\text{THF})$: (i) the spectra in Figure 4 show that Fp reacts without any corresponding increase in the absorbance of the bands due to $\text{Cp}_2\text{Fe}_2(\text{CO})_3(\text{THF})$ and (ii) separate TRIR experiments with visible flash photolysis (510 nm, dye laser)³⁸ show a substantial decrease in the yield of $\text{Cp}_2\text{Fe}_2(\text{CO})_3(\text{THF})$ compared to the UV experiment but little or no change in the yield of Fp.

One might expect $\text{Cp}_2\text{Fe}_2(\text{CO})_3(\text{THF})$ to be formed via $\text{Cp}_2\text{Fe}_2(\text{CO})_3$, by analogy with the formation¹⁹ of $\text{Cp}_2\text{Fe}_2(\text{CO})_3(\text{MeCN})$. However, the spectra in Figure 4 show that $\text{Cp}_2\text{Fe}_2(\text{CO})_3$ is not a precursor to $\text{Cp}_2\text{Fe}_2(\text{CO})_3(\text{THF})$. Nevertheless, the production of $\text{Cp}_2\text{Fe}_2(\text{CO})_3$ and $\text{Cp}_2\text{Fe}_2(\text{CO})_3(\text{THF})$ appear to be linked to the same photochemical pathway. TRIR with visible flash photolysis (510 nm) causes the IR bands of $\text{Cp}_2\text{Fe}_2(\text{CO})_3$ and $\text{Cp}_2\text{Fe}_2(\text{CO})_3(\text{THF})$ to be reduced in intensity (compared to 308-nm photolysis) by similar amounts.³⁸ Furthermore, increasing the concentration of THF in the solution causes an increased yield of $\text{Cp}_2\text{Fe}_2(\text{CO})_3(\text{THF})$ (not illustrated) with a corresponding decrease in the yield of $\text{Cp}_2\text{Fe}_2(\text{CO})_3$, see Figure 5a. Normally, the lifetime of $\text{Cp}_2\text{Fe}_2(\text{CO})_3$ is quite sensitive to the presence of added ligands (i.e., a concentration of CH_3CN of 6×10^{-3} M reduces the half-life from >0.5 s to only 150 μs).¹⁹ However, what is particularly surprising about the traces in Figure 5a is that, on a ms time scale, relatively high concentrations of THF > 5 M, have no apparent effect on the lifetime of $\text{Cp}_2\text{Fe}_2(\text{CO})_3$ even though the overall yield of $\text{Cp}_2\text{Fe}_2(\text{CO})_3$ is substantially reduced. There are a number of possible explanations for this phenomenon.

(i) The reduced yield of $\text{Cp}_2\text{Fe}_2(\text{CO})_3$ could be the effect of secondary photolysis or of a multiphoton process. This explanation is unlikely, however, because the relative yields of $\text{Cp}_2\text{Fe}_2(\text{CO})_3$ and $\text{Cp}_2\text{Fe}_2(\text{CO})_3(\text{THF})$, for a given concentration of THF, do

(37) $\text{Cp}_2\text{Fe}_2(\text{CO})_3(\text{MeCN})$ has two $\nu(\text{C}-\text{O})$ bands,¹⁹ one terminal at 1945 cm^{-1} and one bridging at 1747 cm^{-1} . $\text{Cp}_2\text{Fe}_2(\text{CO})_3(\text{THF})$ has two $\nu(\text{C}-\text{O})_{\text{terminal}}$ bands, possibly due to cis and trans isomers.

(38) $[\text{CpFe}(\text{CO})_2]_2$ was photolyzed in a 9:1 mixture of *n*-heptane and THF, first with 308 nm then 510 nm, and the TRIR signals of $[\text{CpFe}(\text{CO})_2]_2$, Fp, $\text{Cp}_2\text{Fe}_2(\text{CO})_3$, and $\text{Cp}_2\text{Fe}_2(\text{CO})_3(\text{THF})$ were recorded, and the intensity of the signals produced using 510-nm photolysis were compared with those obtained at 308 nm. When the signals had been normalized to allow for the reduced depletion of $[\text{CpFe}(\text{CO})_2]_2$ with 510 nm, the yield of Fp was found to be unchanged, while the yields of $\text{Cp}_2\text{Fe}_2(\text{CO})_3$ and $\text{Cp}_2\text{Fe}_2(\text{CO})_3(\text{THF})$ fell by 65% and 75%, respectively.²⁵

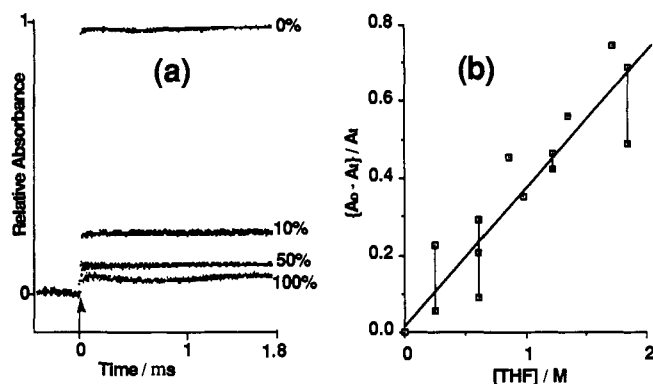
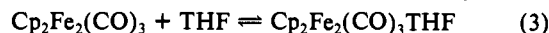


Figure 5. (a) TRIR kinetic traces (1823 cm^{-1} , Xe flash lamp photolysis) showing the generation of $\text{Cp}_2\text{Fe}_2(\text{CO})_3$ in cyclohexane containing different concentrations of THF under an Ar atmosphere. The traces are labeled with the concentration of THF, % by volume. (b) Plot of $\{A_0 - A_T\}/A_T$ vs $[\text{THF}]$ where A refers to the absorbance values of the appropriate TRIR signals due to the $\nu(\text{C}-\text{O})_{\text{bridging}}$ band of $\text{Cp}_2\text{Fe}_2(\text{CO})_3$ obtained by 308-nm laser photolysis of solutions containing up to 15% THF by volume. For a more detailed explanation of the plot see ref 42.

not show a dependence on either the wavelength or intensity of the photolysis source. Similar results are observed with either 308 or 510 nm lasers (<30 ns pulse) or with a Xe flash lamp (ca. 15 μs FWHM).

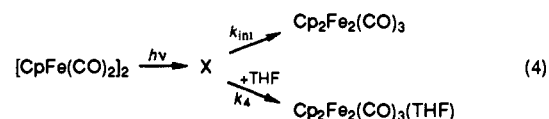
(ii) In low-temperature matrices, $\text{Cp}_2\text{Fe}_2(\text{CO})_3$ is only generated^{5,6} by the photolysis of the trans isomer of $[\text{CpFe}(\text{CO})_2]_2$. In solution, THF is known¹ to reduce the equilibrium concentration of the trans isomer of $[\text{CpFe}(\text{CO})_2]_2$ relative to the cis. If the photochemistry in solution were the same as in the matrix, reduction in the concentration of the trans isomer should lead to a reduction in the yield of $\text{Cp}_2\text{Fe}_2(\text{CO})_3$. However, the suppression of $\text{Cp}_2\text{Fe}_2(\text{CO})_3$ is almost complete in a solution containing 50% THF (see Figure 5a) where the cis/trans ratio¹ is ca. 5:4, and, even in pure THF, the ratio is only 7:3.

(iii) The effect could be due to a rapid equilibrium; increasing the concentration of THF in the solution would then lead to a corresponding increase in the observed amount of $\text{Cp}_2\text{Fe}_2(\text{CO})_3(\text{THF})$, eq 3. This explanation, however, seems improbable.



The relative intensities of the IR bands in Figure 4 indicate that, if this equilibrium existed, the equilibrium constant would be close to unity. Such a value would imply that addition of THF to the formally unsaturated complex, $\text{Cp}_2\text{Fe}_2(\text{CO})_3$, was an almost thermoneutral process, quite unlikely even for a ligand as weak as THF. Furthermore, the reactions in eq 3 would be expected to be slow since they probably involve a spin change; $\text{Cp}_2\text{Fe}_2(\text{CO})_3(\text{THF})$ will be diamagnetic, while $\text{Cp}_2\text{Fe}_2(\text{CO})_3$ should have a similar triplet ground state to that observed⁷ in $(\text{C}_5\text{Me}_5)_2\text{Fe}_2(\text{CO})_3$. Finally, those addition reactions of $\text{Cp}_2\text{Fe}_2(\text{CO})_3$ which have so far been studied quantitatively,^{19,29} all have similar, and relatively high, enthalpies of activation, ca. 23–28 kJ mol^{-1} .

(iv) A more probable explanation, therefore, is that photoejection of CO from $[\text{CpFe}(\text{CO})_2]_2$ initially leads to a short-lived intermediate, X, which can either isomerize to $\text{Cp}_2\text{Fe}_2(\mu\text{-CO})_3$ or, in the presence of high concentrations of THF, be trapped as $\text{Cp}_2\text{Fe}_2(\text{CO})_3(\text{THF})$, eq 4. There are two reasons for supposing



that the intermediate X must be short-lived. Firstly, laser flash photolysis experiments^{25,39} with UV-visible detection confirm that $\text{Cp}_2\text{Fe}_2(\text{CO})_3$ is formed within 10 ns of the UV flash and some preliminary picosecond results⁴⁰ indicated the appearance of a

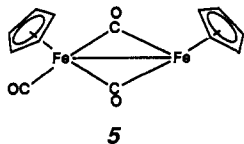
(39) George, M. W., unpublished results.

(40) Peters, K. S., personal communication, 1985.

transient absorption (λ_{max} 510 nm) within 20 ps.⁴¹ Secondly, significant suppression of $\text{Cp}_2\text{Fe}_2(\text{CO})_3$ requires concentrations of THF (ca. 1 M) which are much higher than those normally used to study the reactions of $\text{Cp}_2\text{Fe}_2(\text{CO})_3$ with other ligands e.g. (CO, MeCN, PR₃, etc.).^{11,19}

We have carried out experiments to establish whether the scheme in eq 4 is reasonable, at least on a semiquantitative level. We have used a simple kinetic model,⁴² which suggests that a plot of $(A_0 - A_T)/A_T$ versus the concentration of THF should have a gradient k_4/k_{int} , where A_0 and A_T are, respectively, the absorbance of the IR band of $\text{Cp}_2\text{Fe}_2(\text{CO})_3$ in the absence of THF and at particular concentration, T , of THF. Figure 5b shows such a plot over a concentration range of 0 to ca. 15% THF (0–2 M). Although the scatter of points is considerable, probably a consequence of rather weak TRIR signals and some uncertainty in the concentration of THF, the correlation is acceptable, 0.95, giving a value, $0.36 \pm 0.1 \text{ M}^{-1}$, for the ratio k_4/k_{int} . This ratio seems quite reasonable. If the half-life, $t_{1/2}$, for the isomerization of X were 20 ps, k_{int} would be $3.5 \times 10^{10} \text{ s}^{-1}$, and, applying the ratio of k_4/k_{int} calculated above, k_4 would be ca. $1 \times 10^{10} \text{ M}^{-1} \text{ s}^{-1}$, close to the diffusion limit for reactions in these solvents (e.g., $1.7 \times 10^{10} \text{ M}^{-1} \text{ s}^{-1}$ for *n*-heptane under these conditions).

Despite some relatively obvious simplifications,⁴² this kinetic analysis indicates that our results are consistent with the existence of a short-lived intermediate, X. All ultrafast TRIR experiments on $[\text{CpFe}(\text{CO})_2]_2$ have, up till now, involved photolysis with visible light,^{12,14} conditions which would be expected to generate X in only very small quantities. There is therefore an urgent need for picosecond TRIR experiments with UV photolysis to attempt to detect this intermediate directly. It would clearly be premature to speculate on the precise structure of X until it has been detected, but one of several possibilities would be the doubly-bridged isomer of $\text{Cp}_2\text{Fe}_2(\text{CO})_3$, 5.



5

(41) TRIR measurements at Nottingham have shown that $\text{Cp}_2\text{Fe}_2(\text{CO})_3$ is formed within 125 ns, the risetime of our fast detection system. Early TRIR results^{9a} which indicated that $\text{Cp}_2\text{Fe}_2(\text{CO})_3$ might be formed relatively slowly (i.e., over 1 μs) appear to have been an artifact, possibly caused by use of an InSb detector at a wavelength very close to its band gap.²⁹

(42) Given the scheme defined in eq 4, we can write

$$d[\text{Cp}_2\text{Fe}_2(\text{CO})_3]/dt = k_{\text{int}}[\text{X}]$$

$$d[\text{Cp}_2\text{Fe}_2(\text{CO})_3(\text{THF})]/dt = k_4[\text{THF}][\text{X}]$$

whence

$$[\text{Cp}_2\text{Fe}_2(\text{CO})_3(\text{THF})]/[\text{Cp}_2\text{Fe}_2(\text{CO})_3] = k_4[\text{THF}]/k_{\text{int}} \quad (\text{i})$$

Assuming that the initial concentration of X generated by the UV flash is independent of the concentration of THF in the solution, we can write

$$[\text{Cp}_2\text{Fe}_2(\text{CO})_3(\text{THF})]_T = [\text{Cp}_2\text{Fe}_2(\text{CO})_3]_0 - [\text{Cp}_2\text{Fe}_2(\text{CO})_3]_T \quad (\text{ii})$$

where the subscript T refers to concentrations observed in the presence of a particular amount of THF and 0 to the concentration observed in the absence of THF. Thus, combining eqs i and ii, we have

$$\{[\text{Cp}_2\text{Fe}_2(\text{CO})_3]_0 - [\text{Cp}_2\text{Fe}_2(\text{CO})_3]_T\}/[\text{Cp}_2\text{Fe}_2(\text{CO})_3]_T = (k_4/k_{\text{int}})[\text{THF}]$$

whence

$$\{A_0 - A_T\}/A_T = (k_4/k_{\text{int}})[\text{THF}] \quad (\text{iii})$$

where A refers to the absorbance values of the appropriate TRIR signals due to the $\nu(\text{C}-\text{O})_{\text{bridging}}$ band of $\text{Cp}_2\text{Fe}_2(\text{CO})_3$. This kinetic model is clearly simplified; it ignores, for example, any possible kinetic difference between intermediates generated from the cis and trans isomers of $[\text{CpFe}(\text{CO})_2]_2$ or the complications which might arise from the presence of vibrationally hot species in the wake of the UV flash. In addition, it should be noted that the rapid equilibrium as outlined in eq 3 would give a linear relationship similar to eq iii because the equilibrium constant, K , could be expressed as

$$K = [\text{Cp}_2\text{Fe}_2(\text{CO})_3(\text{THF})]/\{[\text{Cp}_2\text{Fe}_2(\text{CO})_3] \times [\text{THF}]\} = \{A_0 - A_T\}/\{A_T[\text{THF}]\}$$

However, such an equilibrium can almost certainly be discounted for the reasons outlined in the main text.

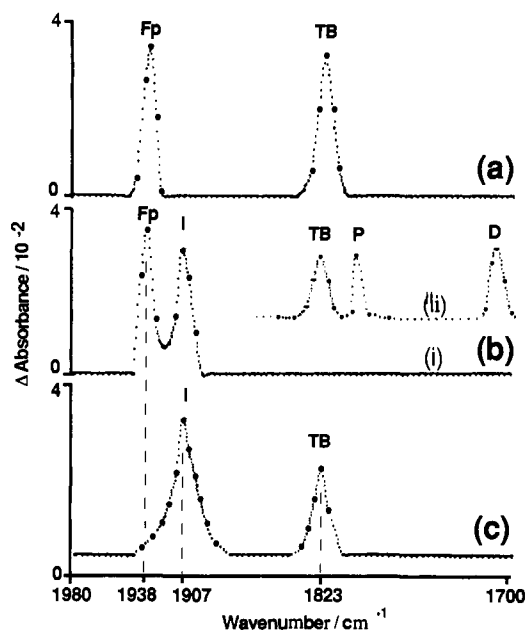


Figure 6. TRIR spectra, Ar-saturated cyclohexane solution, corresponding to 5 μs after UV photolysis (Xe flashlamp) of (a) $[\text{CpFe}(\text{CO})_2]_2$ ($5 \times 10^{-4} \text{ M}$) (b) $\text{Cp}_2\text{Fe}_2(\text{CO})_3\text{P}(\text{OMe})_3$ ($9 \times 10^{-4} \text{ M}$), and (c) $[\text{CpFe}(\text{CO})_2]_2$ in the presence of $\text{P}(\text{OMe})_3$ (10^{-3} M). Bands are labeled as follows: $\text{CpFe}(\text{CO})_2$, Fp; $\text{CpFe}(\text{CO})\text{P}(\text{OMe})_3$, I; $\text{Cp}_2\text{Fe}_2(\text{CO})_3$, TB; $[\text{CpFe}(\text{CO})_2]_2$, P; $[\text{CpFe}(\text{CO})\text{P}(\text{OMe})_3]_2$, D. Note that $\text{Cp}_2\text{Fe}_2(\text{CO})_3$ is not a primary photoproduct of $\text{P}(\text{OMe})_3$ but it is observed on longer time scales as in spectrum b(ii) which corresponds to a time of 50 μs after the flash. $\nu(\text{C}-\text{O})_{\text{terminal}}$ bands due to species destroyed by the flash lie outside the wavenumber range of this figure, and the corresponding $\nu(\text{C}-\text{O})_{\text{bridging}}$ bands have been omitted for clarity.

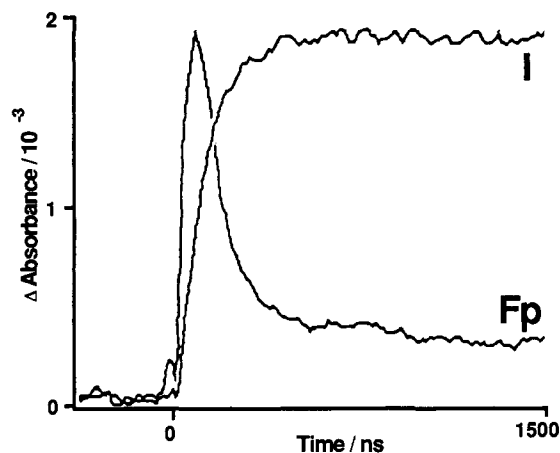


Figure 7. Fast nanosecond TRIR traces obtained by 355-nm photolysis of $[\text{CpFe}(\text{CO})_2]_2$ ($5 \times 10^{-5} \text{ M}$) and $\text{P}(\text{OMe})_3$ ($1.4 \times 10^{-2} \text{ M}$). The traces show the formation and decay of the Fp radical, monitored at 2007 cm^{-1} , and the corresponding growth of the $\text{CpFe}(\text{CO})\text{P}(\text{OMe})_3$ radical, trace labeled I, monitored at 1907 cm^{-1} . (Traces were recorded at Northwestern University.)

These results have implications for reactions with ligands other than THF. In particular, it would appear that, with high concentrations of incoming ligands (e.g., pure MeCN), substitution might occur via direct addition to the intermediate X as well as via $\text{Cp}_2\text{Fe}_2(\text{CO})_3$, the route already identified by TRIR. Of course, this would only be expected to accelerate the rate but not to affect the yield of a reaction since X is itself postulated to be the precursor to $\text{Cp}_2\text{Fe}_2(\text{CO})_3$. In the case of reaction with $\text{P}(\text{OR})_3$, however, this rapid pathway is unlikely to be important since the reaction has usually been studied with relatively low concentrations of phosphite, typically 10^{-4} – 10^{-2} M .

Reactions with $\text{P}(\text{OMe})_3$. Figure 6 illustrates three TRIR spectra corresponding to a time of 5 μs after the UV flash pho-

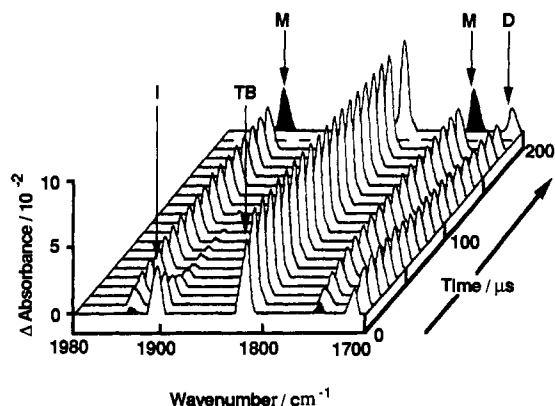
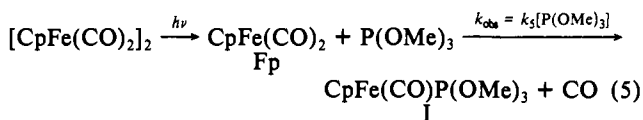


Figure 8. TRIR spectra obtained after the UV flash photolysis (308 nm) of $[\text{CpFe}(\text{CO})_2]_2$ (7×10^{-4} M) in Ar-saturated cyclohexane in the presence of $\text{P}(\text{OMe})_3$ (1×10^{-3} M). Bands are labeled as follows: $\text{CpFe}(\text{CO})\text{P}(\text{OMe})_3$, I; $\text{Cp}_2\text{Fe}_2(\text{CO})_3$, TB; $\text{Cp}_2\text{Fe}_2(\text{CO})_3\text{P}(\text{OMe})_3$, M; $[\text{CpFe}(\text{CO})\text{P}(\text{OMe})_3]_2$, D. As in Figure 4, bands due to the parent $[\text{CpFe}(\text{CO})_2]_2$ and the penultimate spectrum in the series have been omitted for clarity.

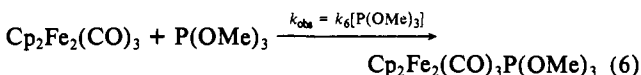
tolysis of (a) $[\text{CpFe}(\text{CO})_2]_2$, (b) $\text{Cp}_2\text{Fe}_2(\text{CO})_3\text{P}(\text{OMe})_3$, and (c) $[\text{CpFe}(\text{CO})_2]_2$ in the presence of $\text{P}(\text{OMe})_3$. Comparison of spectra (a) and (c) shows that, when $\text{P}(\text{OMe})_3$ is present, a new species I is formed at the expense of the Fp radical.⁴³ I is also formed together with the Fp radical during the photolysis of $\text{Cp}_2\text{Fe}_2(\text{CO})_3\text{P}(\text{OMe})_3$, spectrum (b). I has a single $\nu(\text{C}-\text{O})_{\text{terminal}}$ band at 1907 cm^{-1} and no $\nu(\text{C}-\text{O})_{\text{bridging}}$ bands. Fast nanosecond TRIR measurements²⁰ have shown that I is formed directly from the Fp radical, which is extremely short-lived in the presence of even relatively low concentrations of $\text{P}(\text{OMe})_3$, Figure 7. These experiments constitute very strong evidence for I being the $\text{CpFe}(\text{CO})\text{P}(\text{OMe})_3$ radical formed from Fp by substitution of a CO group, eq 5. As previously reported,²⁰ this reaction has an as-



sociative rather than dissociative mechanism with a rate constant, $k_5 = 8.9 \pm 2.0 \times 10^8 \text{ M}^{-1} \text{ s}^{-1}$, not much slower than the diffusion-controlled limit.

Figure 8 shows a series of TRIR spectra obtained during the UV flash photolysis of $[\text{CpFe}(\text{CO})_2]_2$ and $\text{P}(\text{OMe})_3$ in cyclohexane. The overall reaction generates both mono- and disubstituted products, $\text{Cp}_2\text{Fe}_2(\text{CO})_3\text{P}(\text{OMe})_3$ and $[\text{CpFe}(\text{CO})\text{P}(\text{OMe})_3]_2$, indicated by the bands labeled M and D, respectively (see Table II for observed wavenumbers). The surprising feature of this reaction is that the disubstituted compound is formed *more rapidly* than the monosubstituted. Thus, although $\text{Cp}_2\text{Fe}_2(\text{CO})_3\text{P}(\text{OMe})_3$ is the major product at the end of the reaction, $[\text{CpFe}(\text{CO})\text{P}(\text{OMe})_3]_2$ predominates in the earlier stages. On this time scale the Fp radical is too short-lived to be observed, so Figure 8 merely shows the transient IR bands of $\text{Cp}_2\text{Fe}_2(\text{CO})_3$, labeled TB, and $\text{CpFe}(\text{CO})\text{P}(\text{OMe})_3$ marked I. However, there is no $\nu(\text{C}-\text{O})_{\text{bridging}}$ band assignable to a $\text{CpFe}(\text{CO})_2(\mu\text{-CO})\text{CpFe}(\text{CO})\text{P}(\text{OMe})_3$ intermediate, 4.

Kinetic traces taken from a separate experiment with UV laser photolysis, Figure 9a, show that $\text{Cp}_2\text{Fe}_2(\text{CO})_3\text{P}(\text{OMe})_3$ is formed by reaction of $\text{Cp}_2\text{Fe}_2(\text{CO})_3$ with $\text{P}(\text{OMe})_3$, eq 6. Under the



(43) When solutions of $[\text{CpFe}(\text{CO})_2]_2$ with, and without, added $\text{P}(\text{OMe})_3$ were photolyzed with a filtered Xe flash lamp ($\lambda > 610 \text{ nm}$), the signals of the Fp radical and I were reduced by almost identical factors (Fp $\times 5.5$ and I $\times 5.7$) compared to the signals obtained with an unfiltered lamp. Under the same conditions, the signal due to $\text{Cp}_2\text{Fe}_2(\text{CO})_3$ was reduced by a factor of $\times 16 \pm 2$. This behavior contrasts to that described above,³⁵ where $\text{Cp}_2\text{Fe}_2(\text{CO})_3(\text{THF})$ was formed at the expense of $\text{Cp}_2\text{Fe}_2(\text{CO})_3$.

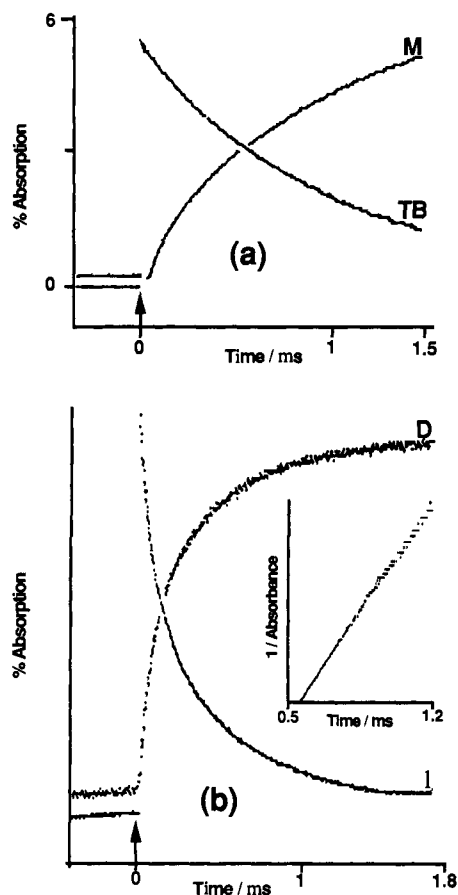
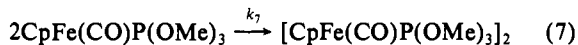


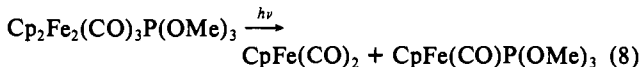
Figure 9. TRIR kinetic traces obtained by 308-nm photolysis of $[\text{CpFe}(\text{CO})_2]_2$ in the presence of $\text{P}(\text{OMe})_3$ (7.8×10^{-3} M). The traces show the formation of (a) $\text{Cp}_2\text{Fe}_2(\text{CO})_3\text{P}(\text{OMe})_3$, labeled M, monitored at 1755 cm^{-1} and the corresponding decay of $\text{Cp}_2\text{Fe}_2(\text{CO})_3$, labeled TB, monitored at 1823 cm^{-1} and (b) the formation of $[\text{CpFe}(\text{CO})\text{P}(\text{OMe})_3]_2$, labeled D, monitored at 1714 cm^{-1} and the corresponding decay of $\text{CpFe}(\text{CO})\text{P}(\text{OMe})_3$, labeled I, monitored at 1907 cm^{-1} . The decay of $\text{CpFe}(\text{CO})\text{P}(\text{OMe})_3$ follows second-order kinetics as shown by the inset plot, $(\text{absorbance})^{-1}$ vs time. Note that in (a) the ordinate of trace TB has been expanded ca. $\times 1.5$ relative to that of trace M.

conditions of our experiment, there is a considerable excess of $\text{P}(\text{OMe})_3$ because UV photolysis causes $<10\%$ depletion of $[\text{CpFe}(\text{CO})_2]_2$. The decay of $\text{Cp}_2\text{Fe}_2(\text{CO})_3$, therefore, follows pseudo-first-order kinetics with k_6 calculated to be $2.7 (\pm 1.0) \times 10^5 \text{ M}^{-1} \text{ s}^{-1}$, a value similar to those observed for reaction of $\text{Cp}_2\text{Fe}_2(\text{CO})_3$ with phosphines,^{19,29} e.g., $2.1 \times 10^5 \text{ M}^{-1} \text{ s}^{-1}$ for PPh_3 . The kinetics of this reaction with PPh_3 have been examined in some detail,²⁹ and it was found, as expected, that the observed rate increased linearly with increasing concentration of PPh_3 over the range 5×10^{-4} – 8×10^{-3} M, but the rate was independent of initial concentration of $[\text{CpFe}(\text{CO})_2]_2$ over the range 1.7×10^{-4} – 1.5×10^{-3} M.

By contrast, $[\text{CpFe}(\text{CO})\text{P}(\text{OMe})_3]_2$ is not formed via $\text{Cp}_2\text{Fe}_2(\text{CO})_3$ rather its growth exactly mirrors the decay of $\text{CpFe}(\text{CO})\text{P}(\text{OMe})_3$, which follows *second-order* kinetics, see inset plot in Figure 9b and eq 7. Evaluating the rate constant, k_7 , for

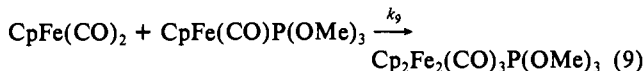


the dimerization of the $\text{CpFe}(\text{CO})\text{P}(\text{OMe})_3$ radical presents exactly the same problem as that encountered with the dimerization of the Fp radical, see above;³³ one requires the value of the IR extinction coefficient of $\text{CpFe}(\text{CO})\text{P}(\text{OMe})_3$. Fortunately, this information can be obtained from the photolysis of $\text{Cp}_2\text{Fe}_2(\text{CO})_3\text{P}(\text{OMe})_3$, which necessarily yields equal quantities of Fp and $\text{CpFe}(\text{CO})\text{P}(\text{OMe})_3$, eq 8. Figure 6b shows the TRIR



spectrum obtained in this way; the IR band of $\text{CpFe}(\text{CO})\text{P}(\text{OMe})_3$ is only slightly less intense than that of Fp. Given the large experimental uncertainty in deriving³³ the extinction coefficient of Fp, it is reasonable to take the extinction coefficients of the two species to be equal, $5.0 \times 10^3 \text{ M}^{-1} \text{ cm}^{-1}$. Applying this value, one obtains $2.0 \times 10^8 \text{ M}^{-1} \text{ s}^{-1}$ as the value of k_7 , the bimolecular rate constant for dimerization of $\text{CpFe}(\text{CO})\text{P}(\text{OMe})_3$.

Thus, TRIR results show formation of $[\text{CpFe}(\text{CO})\text{P}(\text{OMe})_3]_2$ follows a radical pathway, eqs 5 and 7, without the involvement of any dinuclear intermediates. This pathway, first suggested²¹ by Abrahamson et al., is similar to that observed for the photochemical formation⁴⁴ of $\text{Mn}_2(\text{CO})_8\text{L}_2$ from $\text{Mn}_2(\text{CO})_{10}$. Of course, such a pathway could in principle also lead to formation of $\text{Cp}_2\text{Fe}_2(\text{CO})_3\text{P}(\text{OMe})_3$, eq 9. However, this process was not



observed in practice in our experiments because there is no free Fp in solution; the concentration of $\text{P}(\text{OMe})_3$ is such that all of the Fp is converted very rapidly to $\text{CpFe}(\text{CO})\text{P}(\text{OMe})_3$. On the other hand, TRIR traces²⁹ obtained from photolysis of $\text{Cp}_2\text{Fe}_2(\text{CO})_3\text{P}(\text{OMe})_3$ in the absence of added $\text{P}(\text{OMe})_3$ (not illustrated) provide a rather imprecise value of k_9 , $3 \times 10^9 \text{ M}^{-1} \text{ s}^{-1}$. Thus, as might be expected, k_9 is somewhat larger than k_7 , the rate constant for dimerization of $\text{CpFe}(\text{CO})\text{P}(\text{OMe})_3$, but marginally smaller than k_2 , the rate constant for dimerization of the Fp radical. The imprecision in k_9 arises because there are several competing reactions.⁴⁵ TRIR spectra on a longer time scale, 50 μs , show the formation of both $[\text{CpFe}(\text{CO})_2]_2$ and $[\text{CpFe}(\text{CO})\text{P}(\text{OMe})_3]_2$, see Figure 6b(ii). Similar results are observed in CW irradiation experiments with conventional FTIR detection.²⁹ This process is essentially the inverse of a crossover experiment by Abrahamson et al. who reported²¹ that photolysis of a mixture of $[\text{CpFe}(\text{CO})_2]_2$ and $[\text{CpFe}(\text{CO})\text{P}(\text{OMe})_3]_2$ led to formation of $\text{Cp}_2\text{Fe}_2(\text{CO})_3\text{P}(\text{OMe})_3$, presumably via the step shown in eq 9. Our CW photolysis experiments²⁹ also confirmed that photolysis of $\text{Cp}_2\text{Fe}_2(\text{CO})_3\text{P}(\text{OMe})_3$ in the presence of excess $\text{P}(\text{OMe})_3$ yields $[\text{CpFe}(\text{CO})\text{P}(\text{OMe})_3]_2$ as the sole product in agreement with previous observations.^{21,22b} Photochemical processes such as these underline the importance of changing the reaction mixture between each photolysis flash in a TRIR experiment; otherwise the accumulation of photoproducts could lead to a bewildering variety of secondary photochemistry.⁴⁶

Reaction with Other Phosphites. Photochemical substitution reactions between $[\text{CpFe}(\text{CO})_2]_2$ and $\text{P}(\text{O}^i\text{Pr})_3$ or $\text{P}(\text{OEt})_3$ are qualitatively different from those with $\text{P}(\text{OMe})_3$; only monosubstituted products, $\text{Cp}_2\text{Fe}_2(\text{CO})_3\text{P}(\text{OR})_3$, can be isolated from the reaction mixture.²² We have used TRIR to examine these reactions because it was a study^{22,23} of the reaction with $\text{P}(\text{O}^i\text{Pr})_3$ which first led to the proposal that the dinuclear species 4 might be an intermediate in the photochemistry of $[\text{CpFe}(\text{CO})_2]_2$. Surprisingly, our TRIR results with $\text{P}(\text{O}^i\text{Pr})_3$ and $\text{P}(\text{OEt})_3$ are little different from those observed with $\text{P}(\text{OMe})_3$, as described above. For both $\text{P}(\text{O}^i\text{Pr})_3$ and $\text{P}(\text{OEt})_3$, TRIR measurements (not illustrated) confirm that the corresponding monosubstituted $\text{Cp}_2\text{Fe}_2(\text{CO})_3\text{P}(\text{OR})_3$ species are formed via $\text{Cp}_2\text{Fe}_2(\text{CO})_3$ as shown for $\text{P}(\text{OMe})_3$ in eq 6 and Figure 9a above. More interesting is the observation that, on a microsecond time scale, the formation of the Fp radical is suppressed by the presence of $\text{P}(\text{O}^i\text{Pr})_3$ in the

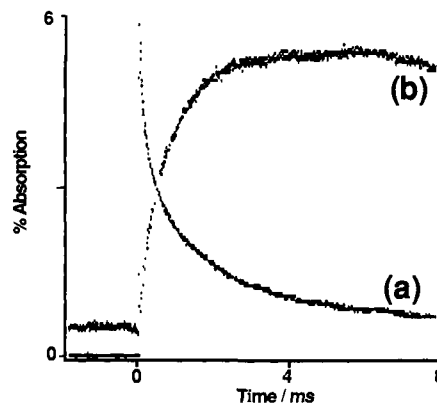
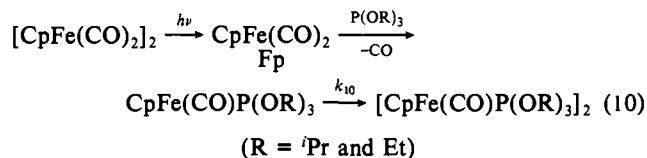


Figure 10. TRIR kinetic traces obtained by 308-nm photolysis of $[\text{CpFe}(\text{CO})_2]_2$ ($5 \times 10^{-4} \text{ M}$) and $\text{P}(\text{O}^i\text{Pr})_3$ (10^{-3} M) in Ar-saturated cyclohexane. The traces show (a) the formation and decay of an absorption at 1904 cm^{-1} , assigned to $\text{CpFe}(\text{CO})\text{P}(\text{O}^i\text{Pr})_3$, and (b) the corresponding growth of the absorption at 1720 cm^{-1} , assigned to $[\text{CpFe}(\text{CO})\text{P}(\text{O}^i\text{Pr})_3]_2$. Note that the ordinate of trace (b) has been expanded ca. $\times 1.7$ relative to that of trace (a).

solution. Instead, one observes a single $\nu(\text{C}-\text{O})_{\text{terminal}}$ band at 1904 cm^{-1} , only 3 cm^{-1} lower than the band due to $\text{CpFe}(\text{CO})\text{P}(\text{OMe})_3$. Figure 10 shows that the TRIR signal at this wavenumber decays by a second-order process at a rate which is exactly matched by the growth of a $\nu(\text{C}-\text{O})_{\text{bridging}}$ band at 1720 cm^{-1} , only 6 cm^{-1} above that of $[\text{CpFe}(\text{CO})\text{P}(\text{OMe})_3]_2$. Very similar results were obtained with $\text{P}(\text{OEt})_3$ except that the maxima of the transient IR signals were at 1907 and 1714 cm^{-1} , respectively. By analogy with the reactions with $\text{P}(\text{OMe})_3$, the most likely interpretation of these observations is that $\text{P}(\text{OR})_3$ reacts rapidly with the Fp radical to generate $\text{CpFe}(\text{CO})\text{P}(\text{OR})_3$ which then dimerizes to generate the previously unknown $[\text{CpFe}(\text{CO})\text{P}(\text{OR})_3]_2$ complexes, eq 10.



Assuming the same value for the IR extinction coefficients of these $\text{CpFe}(\text{CO})\text{P}(\text{OR})_3$ species as that of Fp and $\text{CpFe}(\text{CO})\text{P}(\text{OMe})_3$, $5 \times 10^3 \text{ M}^{-1} \text{ cm}^{-1}$, the rate constant for dimerization of $\text{CpFe}(\text{CO})\text{P}(\text{OR})_3$, k_{10} , has values of 9.0×10^6 (^iPr) and $1.4 \times 10^6 \text{ M}^{-1} \text{ s}^{-1}$ (Et). Thus, the value of k_{10} (^iPr) is about one order of magnitude less than that of k_{10} (Et), which is close in value to k_7 , the corresponding rate constant for $\text{CpFe}(\text{CO})\text{P}(\text{OMe})_3$. k_7 is, in turn, about an order of magnitude less than k_2 , the rate constant for dimerization of the Fp radical, see above. This trend is consistent with the steric bulk of the phosphite and is similar to the trends previously reported⁴⁷ for the rate of dimerization of $\text{Mn}(\text{CO})_4\text{PR}_3$ radicals.

Although the TRIR signals of $[\text{CpFe}(\text{CO})\text{P}(\text{OR})_3]_2$ (1720 cm^{-1} , $\text{P}(\text{O}^i\text{Pr})_3$; 1714 cm^{-1} , Et) are stable on a millisecond time scale, no bands are present at these wavenumbers in FTIR spectra recorded some minutes after photolysis of the solutions.^{22,29} Presumably these $[\text{CpFe}(\text{CO})\text{P}(\text{OR})_3]_2$ compounds are relatively labile, undergoing facile homolysis of the M-M bond in a manner similar to that observed⁴⁸ for $[\text{CpCr}(\text{CO})_3]_2$.

Thus, our TRIR study shows that the photochemical reaction between $[\text{CpFe}(\text{CO})_2]_2$ and $\text{P}(\text{O}^i\text{Pr})_3$ can be explained without invoking the $\text{CpFe}(\text{CO})_2(\mu\text{-CO})\text{CpFe}(\text{CO})\text{P}(\text{O}^i\text{Pr})_3$ intermediate, 4. However, the $\nu(\text{C}-\text{O})_{\text{bridging}}$ band of $[\text{CpFe}(\text{CO})\text{P}(\text{O}^i\text{Pr})_3]_2$ in cyclohexane solution is at exactly the same wavenumber (1720 cm^{-1}) as that reported by Tyler and co-workers²² for their yellow

(44) Byers, B. H.; Brown, T. L. *J. Am. Chem. Soc.* **1977**, *99*, 2527. Herrinton, T. R.; Brown, T. L. *J. Am. Chem. Soc.* **1985**, *107*, 5700.

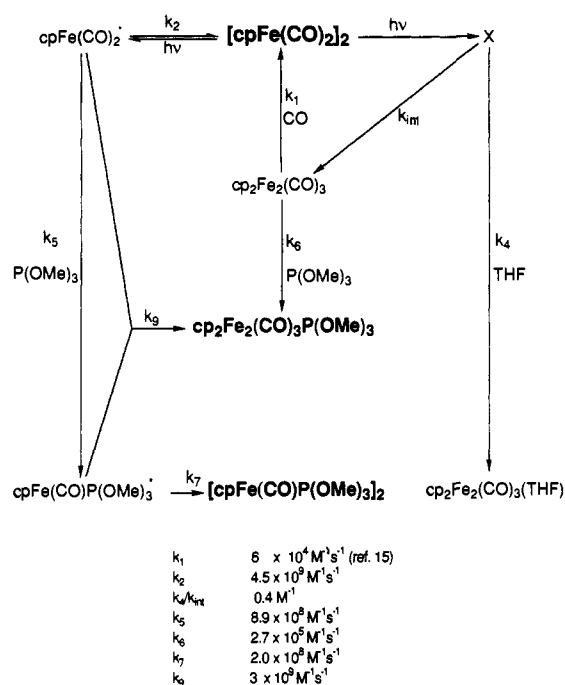
(45) There is an interesting and so far unexplained feature of the photolysis of $\text{Cp}_2\text{Fe}_2(\text{CO})_3\text{P}(\text{OMe})_3$, namely that $\text{Cp}_2\text{Fe}_2(\mu\text{-CO})_3$ is formed but not as a primary photoproduct, see Figure 6b. Since we have already shown (see above) that any intermediate in the formation of $\text{Cp}_2\text{Fe}_2(\mu\text{-CO})_3$ must be extremely short-lived, the relatively slow formation of $\text{Cp}_2\text{Fe}_2(\mu\text{-CO})_3$ in Figure 6 is probably due to one of the primary photoproducts, Fp or $\text{CpFe}(\text{CO})\text{P}(\text{OMe})_3$, reacting with excess $\text{Cp}_2\text{Fe}_2(\text{CO})_3\text{P}(\text{OMe})_3$.

(46) Indeed, multiple shot UV photolysis of $[\text{CpFe}(\text{CO})_2]_2$ and $\text{P}(\text{OMe})_3$ in cyclohexane (i.e., repeated firing of the UV laser without changing the solution) gives rise to an unidentified transient species with two $\nu(\text{C}-\text{O})_{\text{terminal}}$ bands at 1977 and 1942 cm^{-1} ; this may be the same species which was observed under an atmosphere of CO, see ref 51 below.

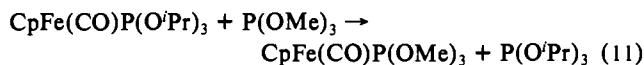
(47) Walker, H. W.; Herrick, R. S.; Olsen, R. J.; Brown, T. L. *Inorg. Chem.* **1984**, *23*, 3748.

(48) Indeed $[\text{CpCr}(\text{CO})_2\text{PPh}_3]_2$ is fully dissociated, and the $\text{CpCr}(\text{CO})_2\text{PPh}_3$ radical has been characterized crystallographically (Cooley, N. A.; Watson, K. A.; Fortier, S.; Baird, M. C. *Organometallics* **1986**, *5*, 2563).

Scheme I



intermediate in THF solution at -78°C and attributed by them to the $\nu(\text{C}-\text{O})_{\text{bridging}}$ band of **4**. It is therefore tempting to suggest that the species which they observed was actually $[\text{CpFe}(\text{CO})\text{P}(\text{O}^i\text{Pr})_3]_2$, the lifetime of which would presumably be extended considerably at low temperatures. Furthermore, one can rationalize their observation²² that the yellow intermediate reacts thermally with $\text{P}(\text{OMe})_3$ to give $[\text{CpFe}(\text{CO})\text{P}(\text{OMe})_3]_2$ (see Introduction above) merely by postulating a relatively rapid phosphite exchange reaction, eq 11.



Similarly, a radical pathway involving $\text{P}(\text{O}^i\text{Pr})_3$ would provide a simple rationalization of the observation²² that, unlike the photochemical reaction of $[\text{CpFe}(\text{CO})_2]_2$ with PPh_3 , formation of $\text{Cp}_2\text{Fe}_2(\text{CO})_3\text{P}(\text{O}^i\text{Pr})_3$ from $[\text{CpFe}(\text{CO})_2]_2$ is not quantitative.

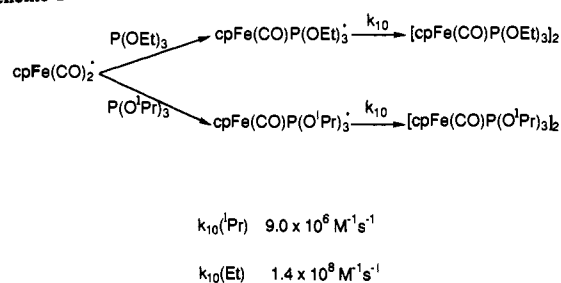
An interesting question, therefore, is why the Fp radical reacts so fast with alkyl phosphites while apparently not reacting at all with alkyl and aryl phosphines.^{4,19,49} In fact, the difference may be quantitative rather than qualitative. We have shown that the reaction between Fp and $\text{P}(\text{OMe})_3$ is associative,²⁰ eq 5, and presumably the reactions with other $\text{P}(\text{OR})_3$ are similar. Such reactions are more sensitive to the nature of the incoming ligand than are the dissociative processes which occur in many organometallic substitution reactions. In these circumstances, it would not be surprising to find a difference between reactivity of Fp toward phosphites and phosphines. Fp dimerizes rapidly (see above) and is relatively short-lived in solution even when quite dilute. Thus, if the rate constants for reaction with phosphines were only a few orders of magnitude smaller than those for reaction with phosphites, the reaction with phosphines would be undetectable under the conditions used in these reactions. This suggestion is consistent with photochemical studies⁵⁰ on $[\eta^5\text{-indenyl}]\text{Fe}(\text{CO})_2]_2$ where the relatively long-lived $(\eta^3\text{-indenyl})\text{-Fe}(\text{CO})_2\text{PPh}_3$ radical is indeed formed, presumably via reaction **3** with the $(\eta^5\text{-indenyl})\text{Fe}(\text{CO})_2$ radical.

There has been considerable argument over the participation of 19-electron species in organometallic reactions such as these.^{22c} Clearly an associative process involving the Fp radical implies the

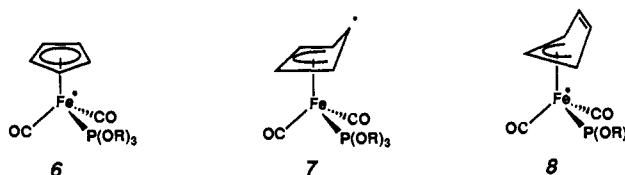
(49) A study of the thermal reactions of $\text{CpFe}(\text{CO})_2(\eta^1\text{-C}_5\text{H}_5)$ has produced evidence for reaction of $[\text{CpFe}(\text{CO})_2]_2$ with PR_3 (Fabian, B. D.; Labinger, J. A. *Organometallics* **1983**, *2*, 659).

(50) Wu, Y.-M.; Zou, C.; Wrighton, M. S. *J. Am. Chem. Soc.* **1987**, *109*, 5861.

Scheme II



existence, at least transiently, of a $\text{CpFe}(\text{CO})_2\text{P}(\text{OR})_3$ intermediate. As in the case of the short-lived intermediate X, postulated in eq 4, it would be premature to discuss the detailed structure of a $\text{CpFe}(\text{CO})_2\text{P}(\text{OR})_3$ intermediate before it has been detected.⁵¹ Clearly, such a species could indeed have a 19-electron configuration, **6**, or it could involve so-called "slippage" of the Cp ring from η^5 to η^4 , **7**, as was observed in low-temperature glasses⁵² or to η^3 , **8**, as was assigned to $(\eta^3\text{-indenyl})\text{Fe}(\text{CO})_2\text{PPh}_3$ on the basis of ESR spectroscopy.⁵⁰ However, it is important to point out that the overall exchange reaction, eq 6, is so fast that any $\text{CpFe}(\text{CO})_2\text{P}(\text{OR})_3$ intermediate must be extremely short-lived and labile, unlike its indenyl analogues, possibly little more than an outer-sphere complex.



Conclusions

This paper demonstrates how time-resolved IR spectroscopy can be used to probe the mechanism of a complex set of organometallic reactions. Schemes I and II summarize the overall mechanism for the substitution reactions of $[\text{CpFe}(\text{CO})_2]_2$ as revealed by our TRIR experiments. There is no evidence for the formation of intermediates of type $\text{CpFe}(\text{CO})_2(\mu\text{-CO})\text{CpFe}(\text{CO})\text{P}(\text{OR})_3$, **4**, which have been postulated as playing an important role in these reactions.²² The photochemical reactions of $[\text{CpFe}(\text{CO})_2]_2$ with PR_3 and $\text{P}(\text{OR})_3$ can be explained on the basis of only three intermediates, $\text{Cp}_2\text{Fe}_2(\text{CO})_3$, $\text{CpFe}(\text{CO})_2$, and $\text{CpFe}(\text{CO})\text{P}(\text{OR})_3$ all of which have been detected in the reaction mixture, and rate constants have been determined for nearly all of the individual steps in the schemes. The only species which has not been detected is the very short-lived intermediate, labeled X in the scheme; the reaction with THF provides circumstantial evidence for its existence but further picosecond TRIR experiments with UV photolysis are required to confirm this. The IR band originally attributed²² to **4** was probably due to $[\text{CpFe}(\text{CO})\text{P}(\text{O}^i\text{Pr})_3]_2$, a species which was originally considered not to be significant in this reaction.

Our recently published study⁵³ of the photocatalytic hydrogenation of norbornadiene demonstrated the importance of combining the results of TRIR experiments with those obtained from other techniques (e.g., matrix isolation, low-temperature solutions,

(51) When $[\text{CpFe}(\text{CO})_2]_2$ is photolyzed under an atmosphere of CO, the TRIR spectrum shows the growth of a secondary product (i.e., well after the end of the UV flash) with two $\nu(\text{C}-\text{O})_{\text{terminal}}$ bands at 1977 and 1942 cm^{-1} . A similar effect is observed in CO matrices at 20 K (Firth, S. Ph.D. Thesis, University of Nottingham, UK, 1986). These bands could be assigned to $\text{CpFe}(\text{CO})_3$ formed by reaction of Fp with CO, but careful measurements show that this assignment was unlikely because the growth of the new species did not match the decay of Fp. A more plausible assignment is to the unbridged isomer of $[\text{CpFe}(\text{CO})_2]_2$, which is reported to have IR bands at 2013, 1973, 1938 cm^{-1} in *n*-heptane (Fischer, R. D.; Vogler, A. *J. Organomet. Chem.* **1967**, *7*, 135). It is not clear, however, why the presence of CO should promote the formation of this unbridged isomer.

(52) Blaha, J. P.; Wrighton, M. S. *J. Am. Chem. Soc.* **1985**, *107*, 2694.

(53) Jackson, S. A.; Hodges, P. M.; Jacke, J.; Poliakoff, M.; Turner, J. J.; Grevels, F.-W. *J. Am. Chem. Soc.* **1990**, *112*, 1221; **1990**, *112*, 1234.

product yields, etc.). The same is equally true of the work described in this paper. Although TRIR has played a key role in unravelling the mechanism of these reactions, the results of many other experiments including the flash photolysis⁴ of $[\text{CpFe}(\text{CO})_2]_2$, the characterization of $\text{Cp}_2\text{Fe}_2(\text{CO})_3$ in low-temperature matrices,^{5,6} and measurements of quantum yields^{21,22b} have been important in constructing the complete mechanism shown in the schemes. The great strength of TRIR, however, is that the narrow line width of $\nu(\text{C}-\text{O})$ bands allows one to monitor each intermediate in real time in the reaction mixture, thus reducing the need to speculate when devising the overall mechanism for a reaction. TRIR has now been applied to the reactions of a number of related dinuclear complexes,⁵³ and we are currently extending this work to establish whether the behavior of $[\text{CpFe}(\text{CO})_2]_2$ is typical of such compounds.

Acknowledgment. We thank SERC, the EC Science Program (Contract ST0007), NATO (Grant No. 900544), the Petroleum Research Fund, administered by the American Chemical Society,

the Paul Instrument Fund of the Royal Society, Müttek GmbH, Perkin-Elmer Ltd., and BP International Ltd for their financial support. We are grateful to Dr. S. Firth, Dr. S. A. Gravelle, Dr. M. A. Healy, Dr. P. M. Hodges, Dr. S. M. Howdle, Ms. M. Jobling, Mr. F. P. Johnson, Dr. B. D. Moore, Professor R. N. Perutz, Professor N. Sheppard, Dr. L. J. Van der Burgt, and Dr. A. H. Wright for their help and advice. We thank Professor E. Weitz, Professor J. M. Kelly, and Dr. C. Long for access to equipment in their laboratories. Finally, we thank Mr. D. R. Dye, Mr. J. G. Gamble, Mr. D. Lichfield, Mr. R. Parsons, Mr. W. E. Porter, and Mr. J. M. Whalley for their continued assistance in developing and building the TRIR equipment at Nottingham.

Registry No. 3, 87985-70-4; $[\text{CpFe}(\text{CO})_2]_2$, 12154-95-9; $\text{CpFe}(\text{CO})_2$, 55009-40-0; $\text{Cp}_2\text{Fe}(\text{CO})_3(\text{THF})$, 138489-71-1; $\text{CpFe}(\text{CO})\text{P}(\text{OMe})_3$, 113843-93-9; $\text{CpFe}(\text{CO})\text{P}(\text{O}^i\text{Pr})_3$, 138489-74-4; $\text{CpFe}(\text{CO})\text{P}(\text{OEt})_3$, 138489-75-5; $\text{Cp}_2\text{Fe}_2(\text{CO})_3\text{P}(\text{OMe})_3$, 33087-08-0; $\text{Cp}_2\text{Fe}_2(\text{CO})_3\text{P}(\text{OEt})_3$, 33057-34-0; $\text{Cp}_2\text{Fe}_2(\text{CO})_3\text{P}(\text{O}^i\text{Pr})_3$, 33218-96-1; $[\text{CpFe}(\text{CO})\text{P}(\text{OMe})_3]_2$, 71579-40-3; $[\text{CpFe}(\text{CO})\text{P}(\text{O}^i\text{Pr})_3]_2$, 138489-72-2; $[\text{CpFe}(\text{CO})\text{P}(\text{OEt})_3]_2$, 138489-73-3.

Polymorphism of 1,3-Phenylene Bis(diselenadiazolyl). Solid-State Structural and Electronic Properties of β -1,3- $[(\text{Se}_2\text{N}_2\text{C})\text{C}_6\text{H}_4(\text{CN}_2\text{Se}_2)]$

A. W. Cordes,^{*,1a} R. C. Haddon,^{*,1b} R. G. Hicks,^{1c} R. T. Oakley,^{*,1c} T. T. M. Palstra,^{1b}
L. F. Schneemeyer,^{1b} and J. V. Waszczak^{1b}

Contribution from the Department of Chemistry and Biochemistry, University of Arkansas, Fayetteville, Arkansas 72701, AT&T Bell Laboratories, Murray Hill, New Jersey 07974, and Guelph Waterloo Centre for Graduate Work in Chemistry, Guelph Campus, Department of Chemistry and Biochemistry, University of Guelph, Guelph, Ontario N1G 2W1, Canada.
Received August 12, 1991

Abstract: The solid-state characterization of a second or β -phase of the 1,3-phenylene-bridged diselenadiazolyl diradical 1,3- $[(\text{Se}_2\text{N}_2\text{C})\text{C}_6\text{H}_4(\text{CN}_2\text{Se}_2)]$ is reported. Crystals of this β -phase are monoclinic, space group $P2_1/n$, with $a = 9.108$ (6), $b = 15.233$ (13), $c = 16.110$ (5) Å, $\beta = 103.37$ (5)°, $Z = 8$. The crystal structure consists of chain-like arrays of discrete dimers (4 per unit cell), although one intradimer Se-Se linkage is notably longer (3.41 Å) than the other three (3.125, 3.196, 3.204 Å). The dimer units lie in chains that are linked by a complex three-dimensional array of Se-Se contacts. Variable-temperature single-crystal conductivity measurements on this phase indicate a band gap of 0.77 eV. Consistent with the conductivity measurements, extended Hückel band structure calculations suggest a relatively isotropic electronic structure.

Introduction

Our interest² in the construction of molecular conductors from neutral π -radicals has prompted us to investigate the use of thiazyl and selenazyl radicals as molecular building blocks. Of the various radical derivatives that have been explored,^{3,4} those based on the

1,2,3,5-dithia- and 1,2,3,5-diselenadiazolyl ring systems are particularly appealing as precursors for new materials.^{5,6} Toward this end we recently described the preparation and solid-state structural and electronic properties of the 1,3- and 1,4-phenylene-bridged bis(dithiadiazolyl) and bis(diselenadiazolyl) diradicals $[(\text{E}_2\text{N}_2\text{C})\text{C}_6\text{H}_4(\text{CN}_2\text{E}_2)]$ **1**⁷ and **2**⁸ (E = S, Se). In the

(1) (a) University of Arkansas. (b) AT&T Bell Laboratories. (c) University of Guelph.

(2) (a) Haddon, R. C. *Nature (London)* **1975**, *256*, 394. (b) Haddon, R. C. *Aust. J. Chem.* **1975**, *28*, 2343.

(3) (a) Wolmershäuser, G.; Schnauber, M.; Wilhelm, T. *J. Chem. Soc., Chem. Commun.* **1984**, 573. (b) Wolmershäuser, G.; Schnauber, M.; Wilhelm, T.; Sutcliffe, L. H. *Synth. Met.* **1986**, *14*, 239. (c) Dormann, E.; Nowak, M. J.; Williams, K. A.; Angus, R. O., Jr.; Wudl, F. *J. Am. Chem. Soc.* **1987**, *109*, 2594. (d) Wolmershäuser, G.; Wortmann, G.; Schnauber, M. *J. Chem. Res. Synop.* **1988**, 358. (e) Wolmershäuser, G.; Johann, R. *Angew. Chem., Int. Ed. Engl.* **1989**, *28*, 920. (f) Hayes, P. J.; Oakley, R. T.; Cordes, A. W.; Pennington, W. T. *J. Am. Chem. Soc.* **1985**, *107*, 1346. (g) Boeré, R. T.; Cordes, A. W.; Hayes, P. J.; Oakley, R. T.; Reed, R. W. *Inorg. Chem.* **1986**, *25*, 2445. (h) Oakley, R. T.; Reed, R. W.; Cordes, A. W.; Craig, S. L.; Graham, J. B. **1987**, *109*, 7745. (i) Boeré, R. T.; French, C. L.; Oakley, R. T.; Cordes, A. W.; Privett, J. A. J.; Craig, S. L.; Graham, J. B. *J. Am. Chem. Soc.* **1985**, *107*, 7710. (j) Awere, E. G.; Burford, N.; Haddon, R. C.; Parsons, S.; Passmore, J.; Waszczak, J. V.; White, P. S. *Inorg. Chem.* **1990**, *29*, 4821. (k) Banister, A. J.; Rawson, J. M.; Clegg, W.; Birkby, S. L. *J. Chem. Soc., Dalton Trans.* **1991**, 1099.

(4) Cordes, A. W.; Haddon, R. C.; Oakley, R. T. In *The Chemistry of Inorganic Ring Systems*; Stuedel, R., Ed.; Elsevier: Amsterdam, 1992.

(5) Vegas, A.; Peréz-Salazar, A.; Banister, A. J.; Hey, R. G. *J. Chem. Soc., Dalton Trans.* **1980**, 1812. (b) Hofs, H.-U.; Bats, J. W.; Gleiter, R.; Hartmann, G.; Mews, R.; Eckert-Maksič, M.; Oberhammer, H.; Sheldrick, G. M. *Chem. Ber.* **1985**, *118*, 3781. (c) Fairhurst, S. A.; Johnson, K. M.; Sutcliffe, L. H.; Preston, K. F.; Banister, A. J.; Hauptmann, Z. V.; Passmore, J. *J. Chem. Soc., Dalton Trans.* **1986**, 1465. (d) Boeré, R. T.; Oakley, R. T.; Reed, R. W.; Westwood, N. P. C. *J. Am. Chem. Soc.* **1989**, *111*, 1180. (e) Banister, A. J.; Hansford, M. I.; Hauptmann, Z. V.; Wait, S. T.; Clegg, W. *J. Chem. Soc., Dalton Trans.* **1989**, 1705. (f) Cordes, A. W.; Goddard, J. D.; Oakley, R. T.; Westwood, N. P. C. *J. Am. Chem. Soc.* **1989**, *111*, 6147.

(6) Del Bel Belluz, P.; Cordes, A. W.; Kristof, E. M.; Kristof, P. V.; Liblong, S. W.; Oakley, R. T. *J. Am. Chem. Soc.* **1989**, *111*, 9276.

(7) Andrews, M. P.; Cordes, A. W.; Douglass, D. C.; Fleming, R. M.; Glarum, S. H.; Haddon, R. C.; Marsh, P.; Oakley, R. T.; Palstra, T. T. M.; Schneemeyer, L. F.; Trucks, G. W.; Tycko, R.; Waszczak, J. V.; Young, K. M.; Zimmerman, N. M. *J. Am. Chem. Soc.* **1991**, *113*, 3559.